Situational assessment of COVID-19 in Australia

Technical Report 22 May 2022 (released 12 August 2022)

Contributors

The University of Melbourne, Melbourne, Australia
James M. McCaw (jamesm@unimelb.edu.au), Robert Moss, David J. Price, Freya M. Shearer (freya.shearer@unimelb.edu.au), Ruarai Tobin

Telethon Kids Institute and Curtin University, Perth, Australia
Nick Golding, Tianxiao Hao, Gerry Ryan

Defence Science and Technology, Department of Defence, Australia
Adeshina Adekunle, Peter Dawson, Mingmei Teo

The University of Adelaide, Adelaide, Australia
Dylan Morris, Joshua V. Ross, Tobin South

Monash University, Melbourne, Australia
Rob Hyndman, Michael Lydeamore, Mitchell O'Hara-Wild

The University of New South Wales, Sydney, Australia
James Wood

Preamble

This is the sixth technical report (released on 12 August 2022) in a series on COVID-19 situational assessment in Australia. Previous reports are available at the following link[1]. The focus of the current report is on COVID-19 situational assessment in Australia for the period from late February 2021 through to 21 November 2021. The report is divided into two sections:

- In Part I, we present time-series estimates of key situational assessment metrics, including state-wide transmission potential (TP), the effective reproduction number (R_{eff}), macro-/micro-distancing behaviour, and the effect of vaccination on transmission potential, for each Australian state/territory up to 21 November 2021.
- In Part II, we report short-term forecasts of daily case incidence produced during the Delta epidemic waves in the Australian Capital Territory (ACT), New South Wales (NSW), and Victoria (VIC).

For the first half of 2021, COVID-19 epidemiology in Australia was characterised by repeated, small incursions (of ancestral virus strains or the Alpha variant) and extended periods of zero local case incidence. The national roll-out of a primary two-dose vaccination course commenced on 21 February 2021. In July 2021, transmission of the Delta variant became established in NSW, followed by VIC, and the ACT, resulting in widespread waves of infection in these jurisdictions and sporadic outbreaks in other jurisdictions. By late November 2021, the initial waves of Delta infection had peaked and were in decline, with epidemic activity stabilising at levels manageable within health system capacity. This report focuses on the period prior to the emergence of the Omicron variant and the ramping up of booster/third dose roll-out (both of which occurred in early December). Omicron-era situational assessment will form the basis of a future technical report.

[1] https://mspgh.unimelb.edu.au/research-groups/centre-for-epidemiology-and-biostatistics-research/modelling-and-simulation/covid-19-national-situational-assessment

Part I: Key situational assessment metrics up to 21 November 2021

As described in Golding et al[2], we use a novel semi-mechanistic model to estimate the ability of SARS-CoV-2 to spread in a population, informed by data on cases, population behaviours and health system effectiveness. In the absence of cases, our method estimates the ability of the virus, if it were present, to spread in a population, which we define as the 'transmission potential'. When the virus is present, our method recovers the effective reproduction number (R_{eff}) and, additionally the deviation between the R_{eff} and the transmission potential. Applying this method provides an estimate of the transmissibility of SARS-CoV-2 in periods of high, low, and zero, case incidence, with a coherent transition in interpretation across changing epidemiological situations.

In 2021, our methods were adapted to incorporate the effects of vaccination and increased transmissibility of the Alpha and Delta variants relative to ancestral strains (methodological details provided in the next section).

We provide time-series estimates of state-wide transmission potential (Figure 1), the effective reproduction number (R_{eff}) of active cases (Figure 2), macro-/micro-distancing behaviour (Figures 5 and 6), the time-to-detection of cases (Figure 7) for each Australian state/territory up to 21 November 2021, based on case data extracted from the Australian National Notifiable Diseases Surveillance System (NNDSS) on 22 November 2021. Finally, we include estimates of the population-level effect of vaccination on transmission potential (Figure 3) for each Australian state/territory, and trends in state-wide transmission potential under the counterfactual assumption in which only vaccination had changed over time (Figure 4).

The above metrics are produced weekly for all jurisdictions according to the Australia National Disease Surveillance Plan for COVID-19[3] (Goal 2, Indicators 2.1–2.3; Goal 11, Indicator 1.1), with public summaries available via the Common Operating Picture[4].

Key methodological updates in 2021

Accounting for the effect of vaccination on transmission potential

We compute the multiplicative effect of vaccination on Component 1 of the SARS-CoV-2 transmissibility model (state-wide transmission potential) using a simple age structured next-generation matrix model. This enables us to capture the effect of heterogeneous (across ages) vaccination coverage on transmission potential, which models the average transmission rate across the whole population. We use data on vaccine coverage by age, dose number, product, and state/territory from the Australian Immunisation Register.

Our approach assumes that the reduction in transmission potential due to vaccination is the same under pre-pandemic conditions as under post-pandemic restrictions and population behaviours. In reality, the effectiveness of vaccination will fluctuate over time as behavioural patterns and contact networks change. Hence our estimates can also be interpreted as the effectiveness of vaccination alone on reducing transmission potential; *i.e.*, the estimated rate of transmission with complete relaxation of restrictions and return to pre-pandemic population behaviour.

Vaccines can impact on multiple aspects of transmission and disease, *e.g.*, on susceptibility to infection, probability of onward transmission, *etc.* Our model incorporates a combined effect

[2] https://doi.org/10.1101/2021.11.28.21264509

[3] Version 2.0, April 2021: https://www.health.gov.au/sites/default/files/documents/2021/04/australian-national-disease-surveillance-plan-for-covid-19.pdf

[4] https://www.health.gov.au/resources/collections/coronavirus-covid-19-common-operating-picture

of protection against infection and onward transmission (assuming infection with the Delta variant) of vaccinated individuals by vaccine product and dose number. Further, we assume a 21-day delay to full protection from a single dose, and a 14-day delay to protection from a second dose (increasing linearly immediately upon vaccination) and that protection does not wane. See the Appendix for details. Note that our methods were updated in late 2021/early 2022 to incorporate emerging data on the waning of vaccine-acquired and infection-acquired immunity over time.

Estimating the relative transmissibility of the Alpha and Delta variants

In January 2021, rapid estimates of the relative transmissibility of the Alpha variant compared with ancestral lineages were made by two groups (not peer-reviewed at the time): the London School of Hygiene and Tropical Medicine (LSHTM) and Imperial College. LSHTM estimated a 31% [27%, 34%] increase in the reproduction number based on their regional time-varying model assuming an average generation interval of 3.6 days[5] and Imperial estimated a 50–75% increase in the reproduction number assuming an average generation interval of 6.5 days[6]. In June 2021, there was significant concern over the further increased transmissibility of the Delta variant relative to Alpha.

These estimates assumed that the increased transmissibility of the Alpha and Delta variants can be represented as a multiplicative increase in R_{eff}. However, the impact of Alpha and Delta on transmissibility are likely to depend on the public health response (*e.g.*, level of restrictions on movement) and population behaviour. We therefore performed an independent analysis of the relative transmissibility of the Alpha variant (week commencing 18 January 2021) and the Delta variant (week commencing 21 June 2021) compared with ancestral lineages in the UK, using:

- data from Public Health England (now the UK Health Security Agency) on secondary attack rates among known contacts of cases over two time periods;
- our model for estimating transmission potential in Australia which separately considers household and non-household rates of transmission;
- data on macro-distancing behaviour (from both the UK and Australia) and mobility and micro-distancing behaviour (from the UK).

Our approach allowed us to directly estimate the impact of Alpha and Delta on the probability of transmission to a contact per unit of contact time, and therefore account for changes in the relative transmissibility of variants between periods of high and low social restrictions. Furthermore, our approach accounts for changes in overall transmissibility due to vaccination and population immunity between the two periods for which we have data. Details are provided in the Appendix.

We estimated increases in transmissibility of Alpha relative to ancestral lineages ranging from 36% [29, 42] under nationwide "stay-at-home" restrictions in Australia in March/April 2020 to 43% [35, 50] for a pre-pandemic baseline (R_0). As of 20 June 2021, we estimated increases in transmissibility of Delta relative to Alpha ranging from 36% [31, 41] in VIC (moderate social restrictions in place) to 39% [34, 44] in NT (no social restrictions in place).

[5] `https://cmmid.github.io/topics/covid19/local-r-sgtf.html`

[6] `https://www.imperial.ac.uk/mrc-global-infectious-disease-analysis/covid-19/report-42-sars-cov-2-variant/`

Time-series outputs of key situational assessment metrics

Figure 1: Estimates of state-wide transmission potential by state/territory as of 21 November 2021 (lighter ribbons = 90% credible intervals; darker ribbons = 50% credible interval). Estimates of transmission potential without vaccination (in grey) are overlaid with estimates of transmission potential accounting for the effect of vaccination (in green) from the start of the vaccination roll-out on 21 February 2021 (blue dashed line). Dashed red vertical lines indicate the date of switch from 0% to 100% of transmission risk from Alpha (27 January) and Delta (7 June). Solid grey vertical lines indicate key dates of implementation of various physical distancing policies.

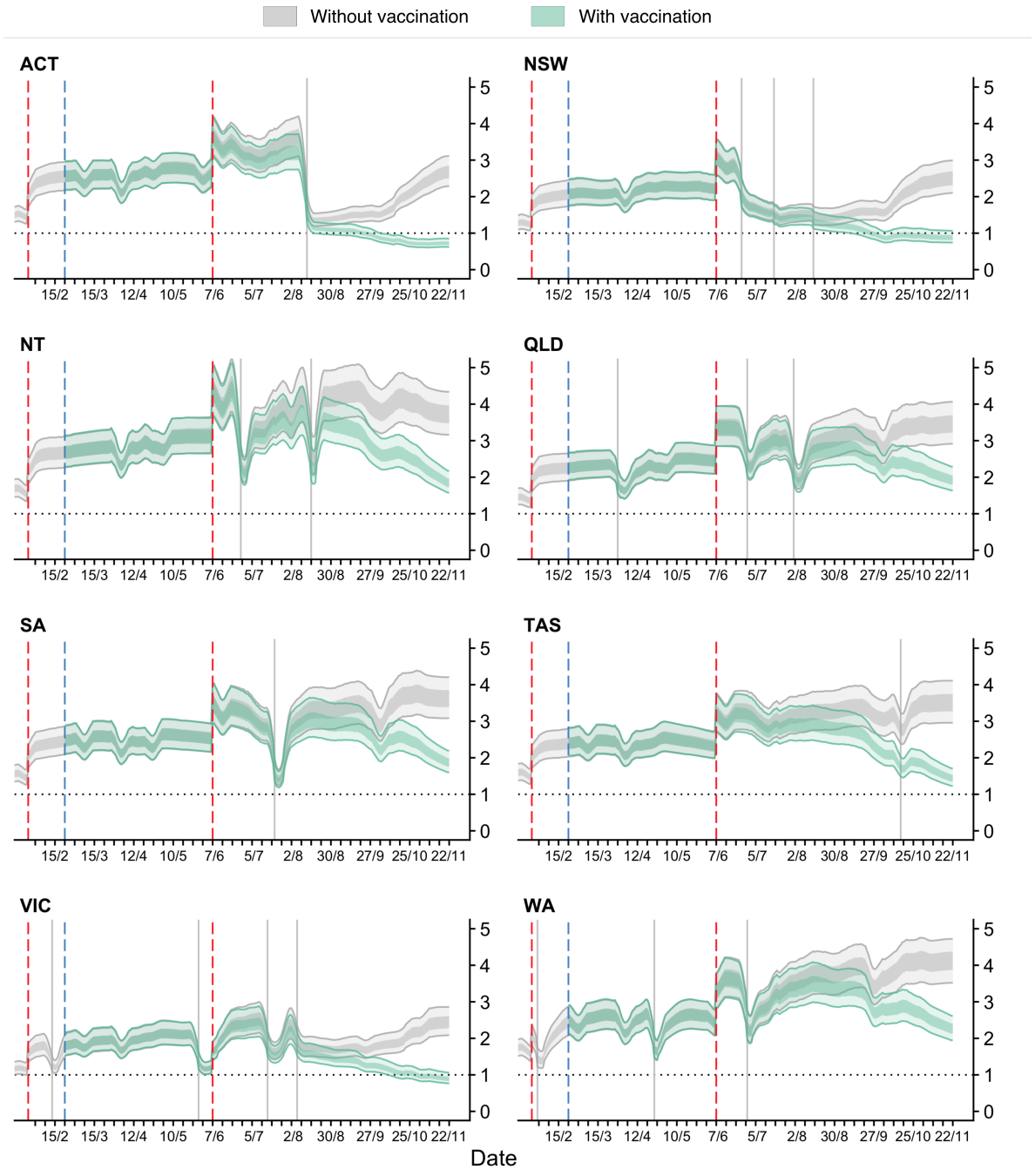

Figure 2: Estimates of R_{eff} for local active cases for each state/territory (light green ribbon = 90% credible interval; dark green ribbon = 50% credible interval). Estimates are made up to 21 November 2021 based on cases with inferred infection dates up to and including 15 November (due to a delay from infection to reporting, the trend in estimates after 15 November is informed by our estimates of R_{eff} up to 15 November and transmission potential). Dashed red vertical lines indicate the date of switch from 0% to 100% of transmission risk from Delta (7 June). Solid grey vertical lines indicate key dates of implementation of various physical distancing policies. Black dotted line indicates the target value of 1 for the effective reproduction number required for control. Local cases by inferred date of infection are indicated by grey ticks on the x-axis. For states/territories and time periods with very low numbers of local active cases, the estimates of R_{eff} for active cases is highly uncertain. The state-wide transmission potential should be referred to when assessing the risk of an epidemic becoming established given a seeding event.

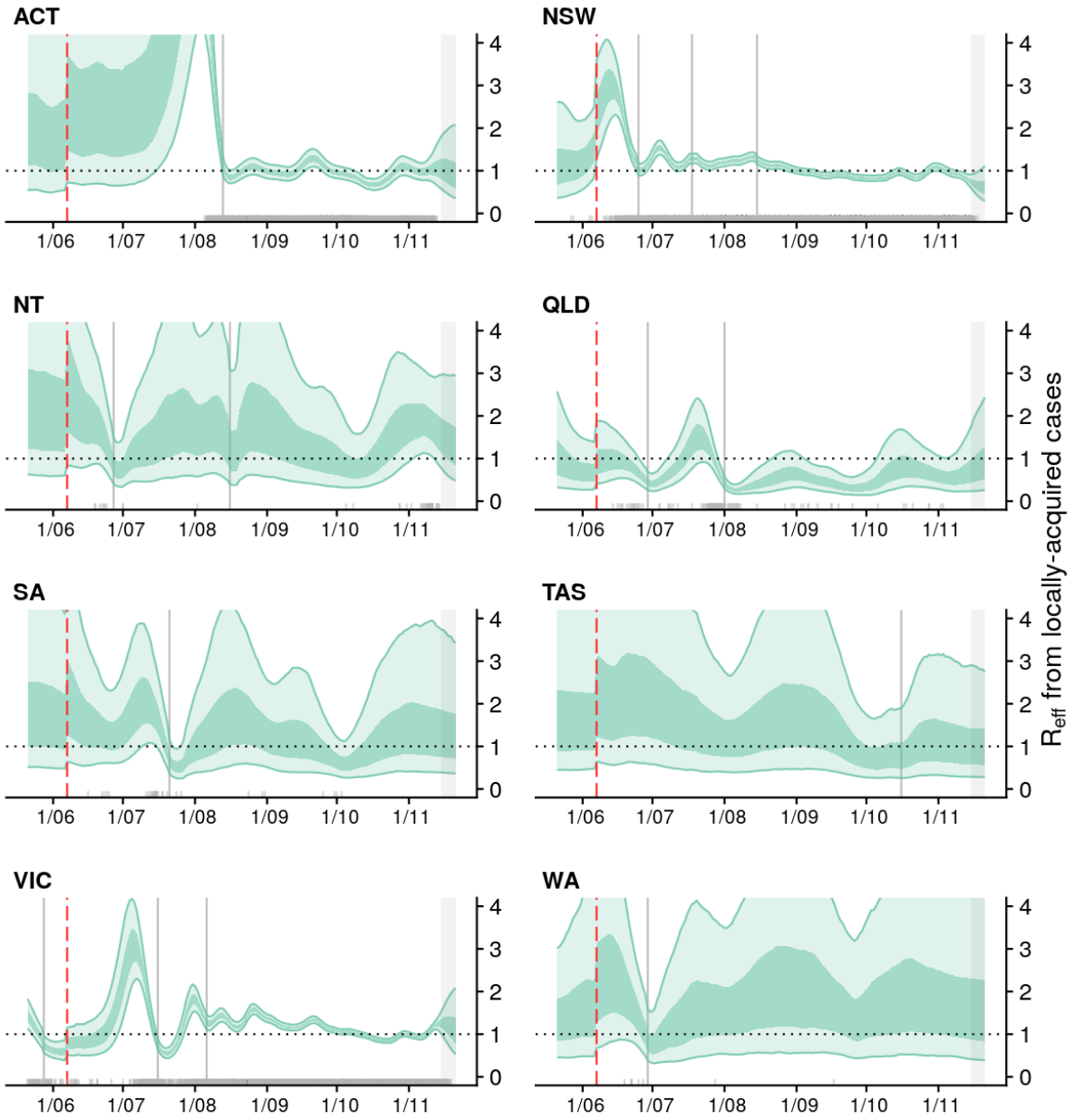

Figure 3: Estimate of the multiplicative effect of vaccination on transmission potential through time by state/territory. As of 21 November 2021, we estimated reductions in transmission potential across states/territories ranging from 44% (QLD) to 73% (ACT). With very high levels of second dose coverage achieved by late November 2021, the effect of vaccination on transmission potential was approaching a maximum achievable value, most evident in ACT, NSW, and VIC. Note that these estimates do not account for the impact of waning of vaccine-acquired immunity.

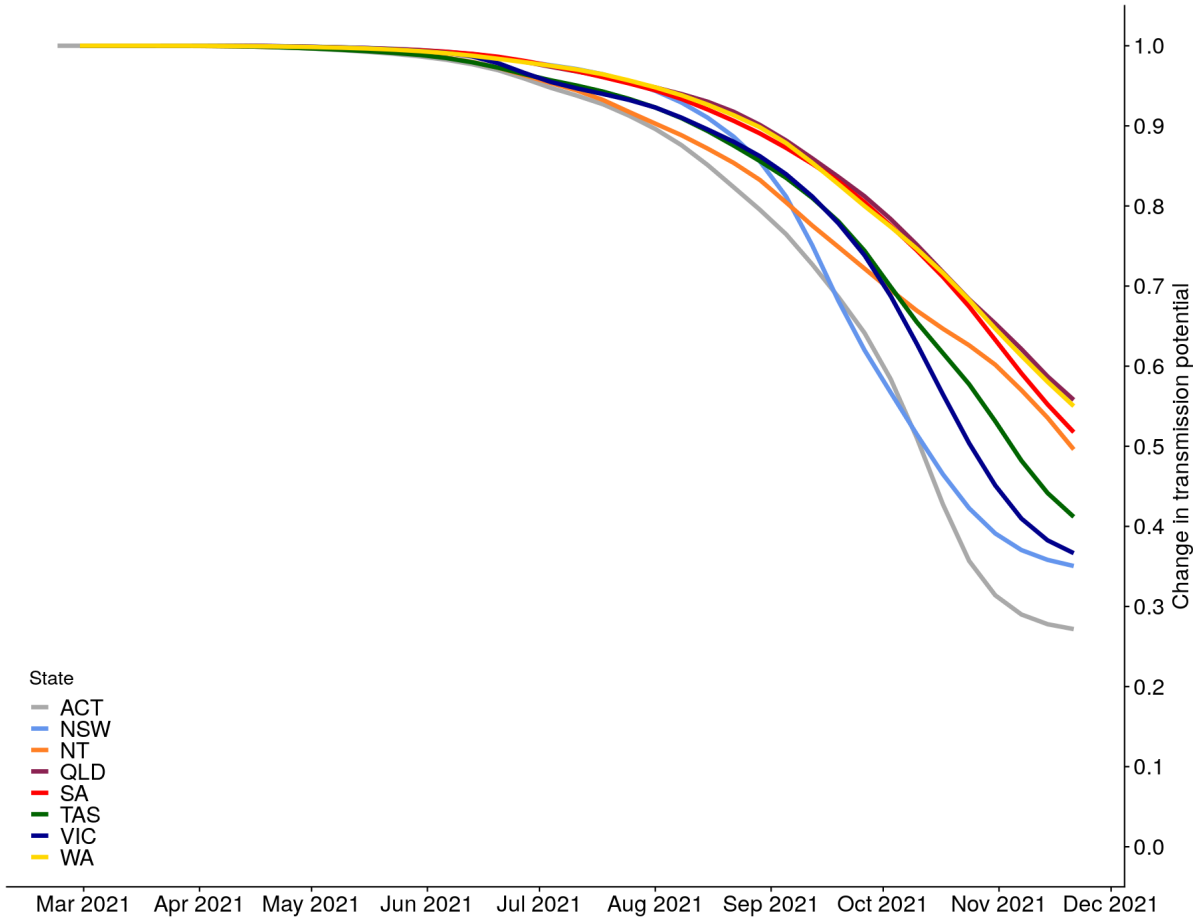

Figure 4: Estimate of state-wide transmission potential by state/territory from 1 March 2020 up to 21 November 2021, if we assume that: only levels of vaccination coverage had changed and not macro-distancing behaviour or micro-distancing behaviour or the time from symptom onset to detection (lighter ribbon = 90% credible interval; darker ribbon = 50% credible interval). Dashed blue vertical line indicates the start of the vaccination roll-out (21 February 2021). Dashed red vertical lines indicate the date of switch from 0% to 100% of transmission risk from Alpha (27 January 2021) and Delta (7 June 2021). Solid grey vertical line indicates the start date of vaccination roll-out. Note that these estimates do not account for the impact of waning of vaccine-acquired immunity.

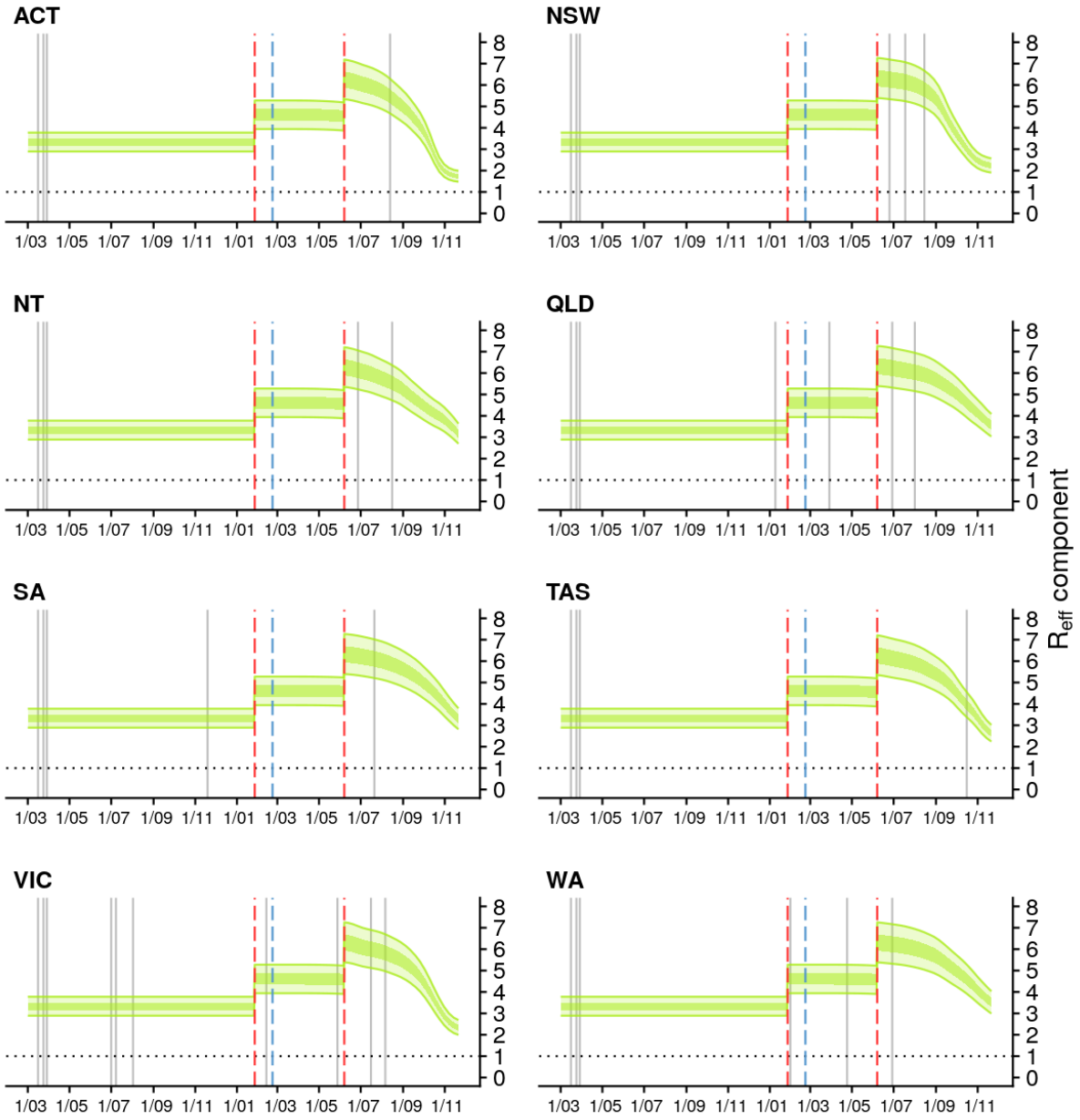

Figure 5: **Estimated trends in macro-distancing behaviour**, *i.e.*, reduction in the daily rate of non-household contacts, from 1 March 2020 up to 21 November 2021 in each state/territory (light purple ribbons = 90% credible intervals; dark purple ribbons = 50% credible intervals). Estimates are informed by state-level data from nationwide surveys (indicated by the black lines and grey rectangles) and population mobility data. The green ticks indicate the dates that public holidays coincided with surveys (when people tend to stay home, biasing down the number of non-household contacts reported on those days).

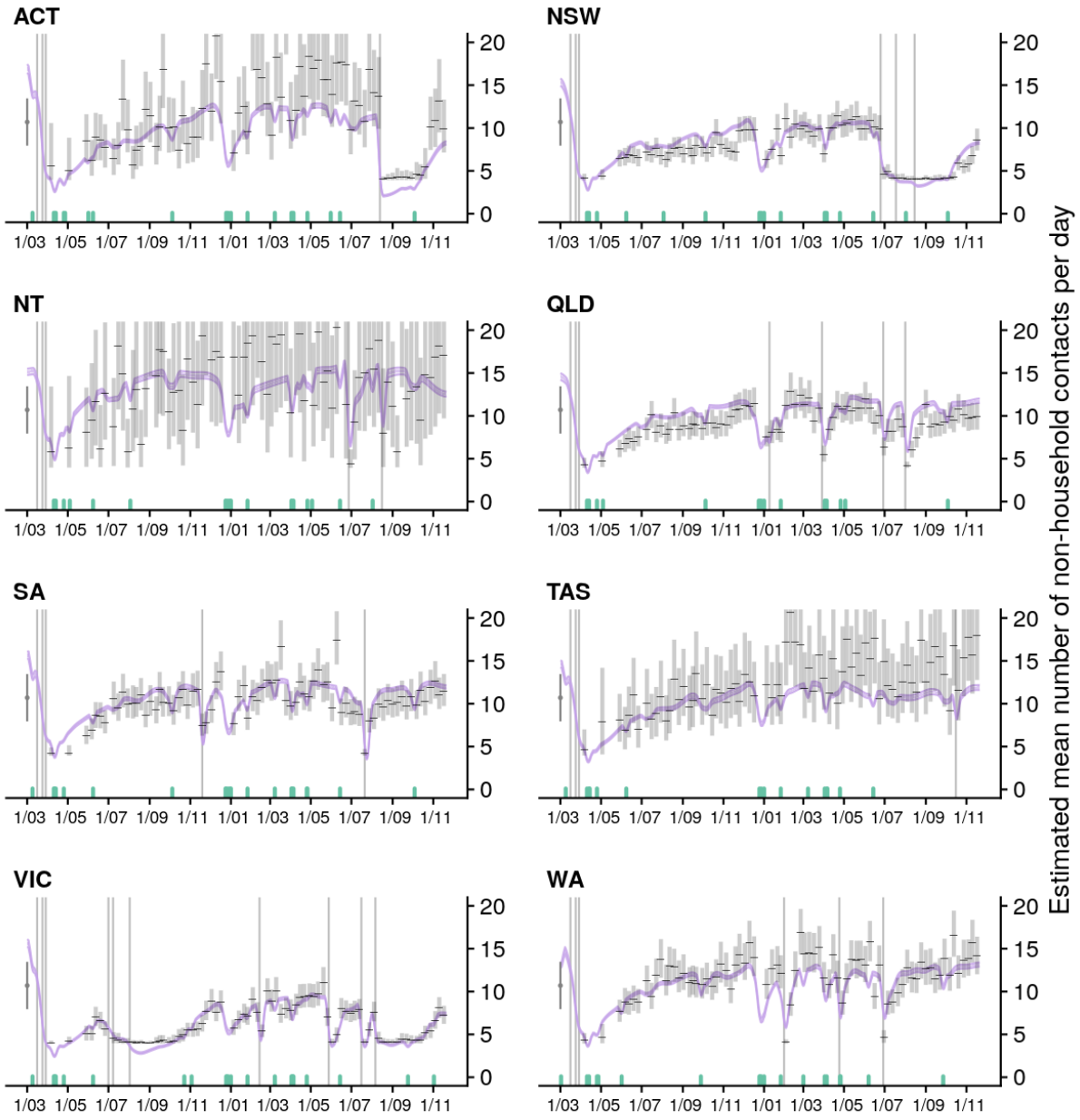

Figure 6: **Estimated trends in micro-distancing behaviour**, *i.e.* reduction in transmission probability per non-household contact, from 1 March 2020 up to 21 November 2021 in each state/territory (light purple ribbons = 90% credible intervals; dark purple ribbons = 50% credible intervals). Estimates are informed by state-level data from nationwide weekly surveys since March 2020 (indicated by the black lines and grey rectangles).

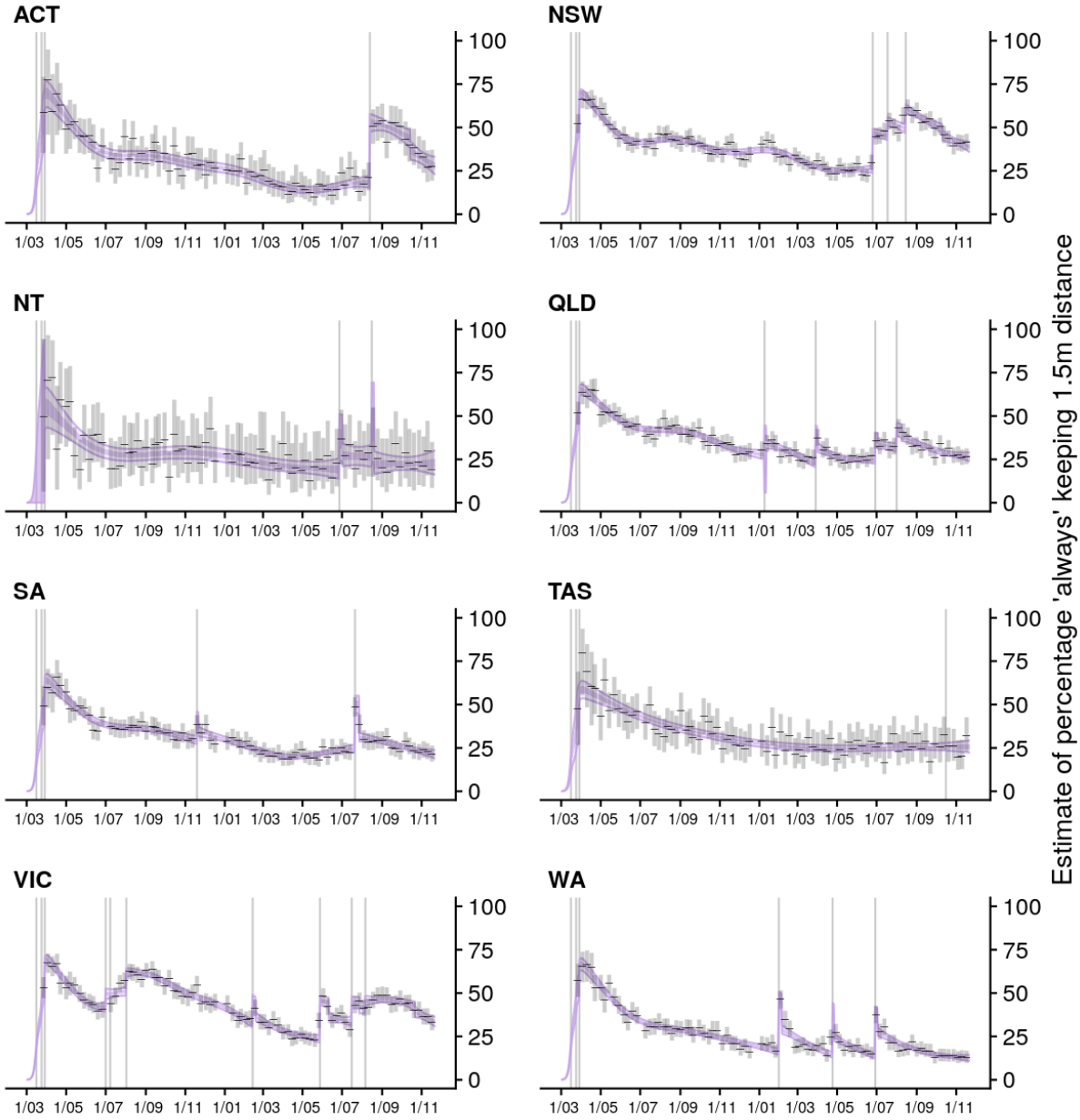

Figure 7: Estimated trend in distributions of time from symptom onset to notification for locally acquired cases for each Australian state/territory from 1 March 2020 to early November 2021 (black line = median; yellow ribbons = 90% distribution quantiles; black dots = time-to-notification of each case). Faded regions indicate where a national trend is used due to low case counts.

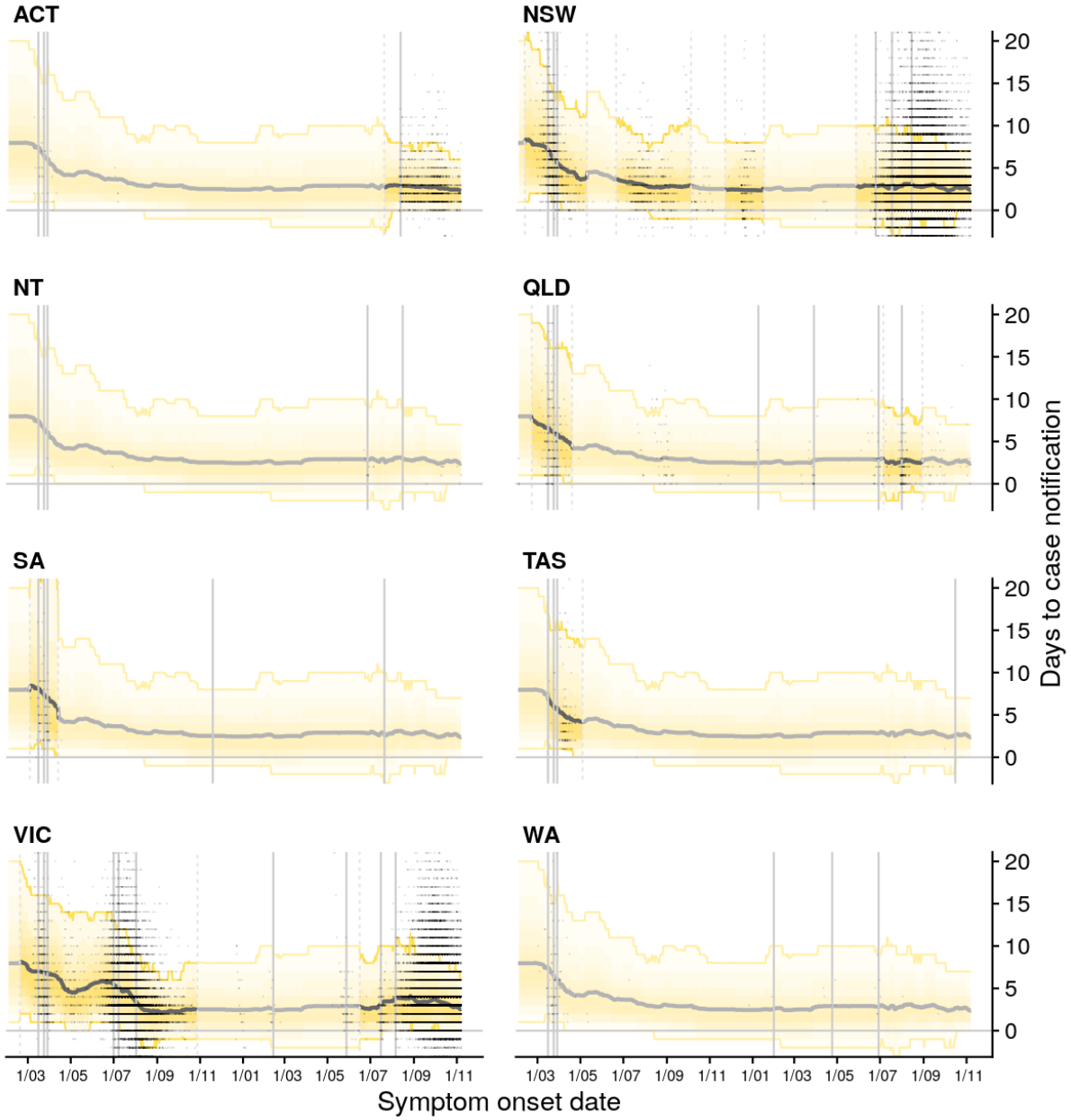

Part II: short-term forecasts of daily case incidence

Forecasts for all jurisdictions are produced weekly according to the Australia National Disease Surveillance Plan for COVID-19[7] (Goal 2, Indicator 2.4). Here we report short-term forecasts of daily case incidence produced over the Delta epidemic waves in the ACT, NSW, and VIC. Weekly forecasts are routinely produced and reported over a four-week horizon. Here we display 7-day (Figure 8), 14-day (Figure 9) and 28-day (Figures 10 and 11) forecasts produced over the period from early July to late November 2021 along with observed daily case counts (as extracted from NNDSS on 1 March 2022). Other states and territories did not have sustained epidemic activity during this period and so forecasts for these jurisdictions are not reported here.

Note that we do not attempt to forecast changes in macro- and micro-distancing behaviour, for example in response to changes in social restrictions, over the forecast horizon.

Overview of methodologies

We report state-level forecasts of the daily number of new confirmed cases from an 'ensemble forecast' of three independent models. Ensemble forecasts tend to produce improved estimates of both the central values, as well as improved estimates of the plausible, yet least likely forecasts (uncertainty). Our ensemble is generated by equally weighting the forecasts from each of the three models. A brief description of each method incorporated in the ensemble is given below, with full methodological detail provided in the Appendix:

- **SEEIIR Forecast**: A stochastic susceptible-exposed-infectious-recovered (SEEIIR) compartmental model that incorporates changes in local transmission potential via the estimated time-varying effective reproduction number (as shown in Figure 2).
- **Probabilistic Forecast**: A stochastic epidemic model that accounts for the number of imported-, symptomatic- and asymptomatic-cases over time. This model estimates the effective reproduction number corresponding to local and imported cases, and incorporates mobility data to infer the effect of macro-distancing behaviour. This model captures variation in the number and timing of new infections via probability distributions. The parameters that govern these distributions are inferred from the case and mobility data (*e.g.*, mean number of imported cases).
- **Time-Series Forecast**: A time-series model that does not account for disease transmission dynamics, but rather uses recent daily case counts to forecast cases into the future. Parameters of this 'autoregressive' model are estimated using global data accessible via the Johns Hopkins COVID-19 repository. Case counts from a specific time window prior to the forecasting date (the present) are used for model calibration. The number of days within this time window is chosen to optimise projections for Australian data.

Accounting for the effects of vaccination

Two of the three models (SEEIIR and Probabilistic) are able to explicitly consider the impact of vaccines on transmission. In the week commencing 7 September 2021, these models were updated to account for effects of the national vaccine roll-out, using data from the Australian Immunisation Register. Full details are provided in the Appendix.

[7] Version 2.0, April 2021: `https://www.health.gov.au/sites/default/files/documents/2021/04/australian-national-disease-surveillance-plan-for-covid-19.pdf`

Figure 8: **7-day projections of new daily local cases** of COVID-19 from the forecasting ensemble for ACT, NSW, and VIC plotted each week from early July to late November 2021 (alternate 7-day periods coloured in purple and blue; darker shading = 50% confidence intervals; lighter shading = 90% confidence intervals). Observed daily counts of locally acquired cases are also plotted from 15 July to 1 December 2021 by date of symptom onset (black dots and lines), based on data extracted from NNDSS on 1 March 2022. Forecasts were fitted to data extracted at the time of analysis (not shown). Due to the time required to update forecasting models to incorporate vaccination, no forecasts were produced in the week commencing 30 August 2021. Due to events such as public holidays, data delays, *etc.*, the forecast start day shifts from week to week, which is why the overlap between forecasts varies.

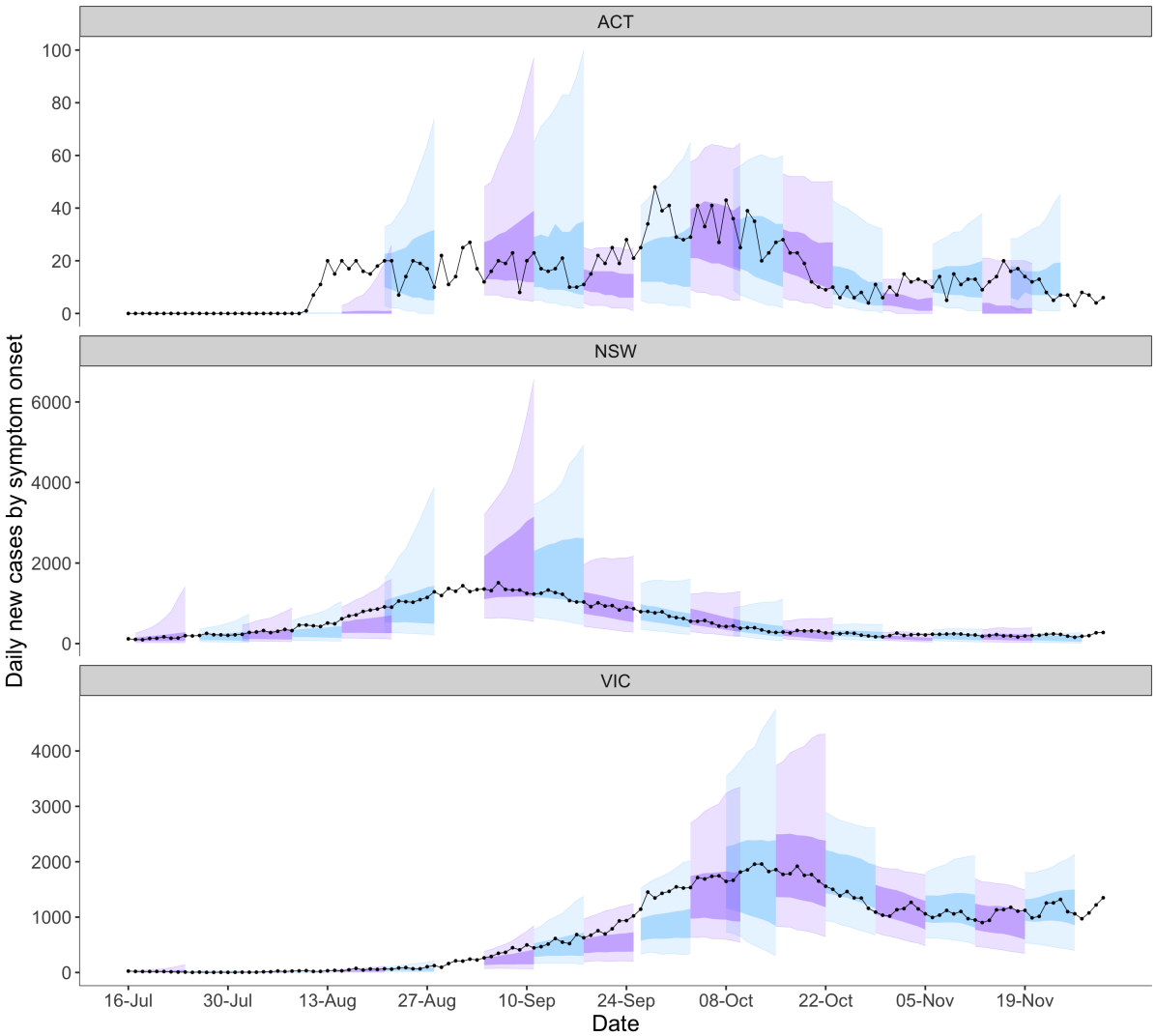

Figure 9: **14-day projections of new daily local cases** of COVID-19 from the forecasting ensemble for ACT, NSW, and VIC plotted every two weeks from early July to late November 2021 (alternate 14-day periods coloured in purple and blue; darker shading = 50% confidence intervals; lighter shading = 90% confidence intervals). Observed daily counts of locally acquired cases are also plotted from 15 July to 1 December 2021 by date of symptom onset (black dots and lines), based on data extracted from NNDSS on 1 March 2022. Forecasts were fitted to data extracted at the time of analysis (not shown). Due to the time required to update forecasting models to incorporate vaccination, no forecasts were produced in the week commencing 30 August 2021. Due to events such as public holidays, data delays, *etc.*, the forecast start day shifts from week to week, which is why the overlap between forecasts varies. Note that every other forecast is shown here, with the alternate set displayed in Figure S1.

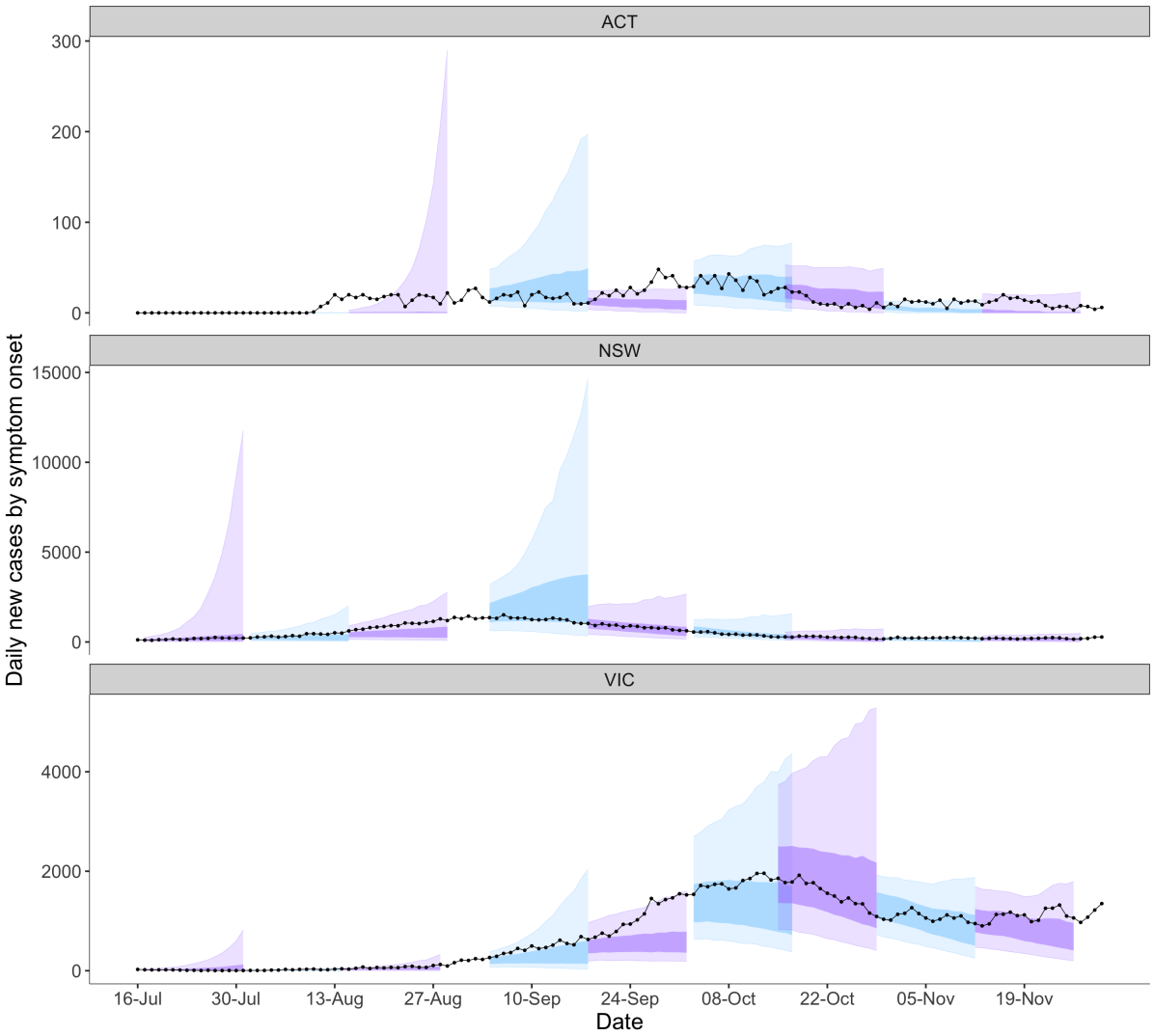

Figure 10: **28-day projections of new daily local cases** of COVID-19 from the forecasting ensemble for ACT, NSW, and VIC plotted every month from early July to late November 2021 (alternate 28-day periods coloured in purple and blue; darker shading = 50% confidence intervals; lighter shading = 90% confidence intervals). Observed daily counts of locally acquired cases are also plotted from 15 July to 1 December 2021 by date of symptom onset (black dots and lines), based on data extracted from NNDSS on 1 March 2022. Forecasts were fitted to data extracted at the time of analysis (not shown). Due to the time required to update forecasting models to incorporate vaccination, no forecasts were produced in the week commencing 30 August 2021. Due to events such as public holidays, data delays, *etc.*, the forecast start day shifts from week to week, which is why the overlap between forecasts varies. Plots with truncated y-axis limits are displayed in Figure 11 below. Note that every fourth forecast is shown here with the alternatives displayed in Figures S2, S3, and S4.

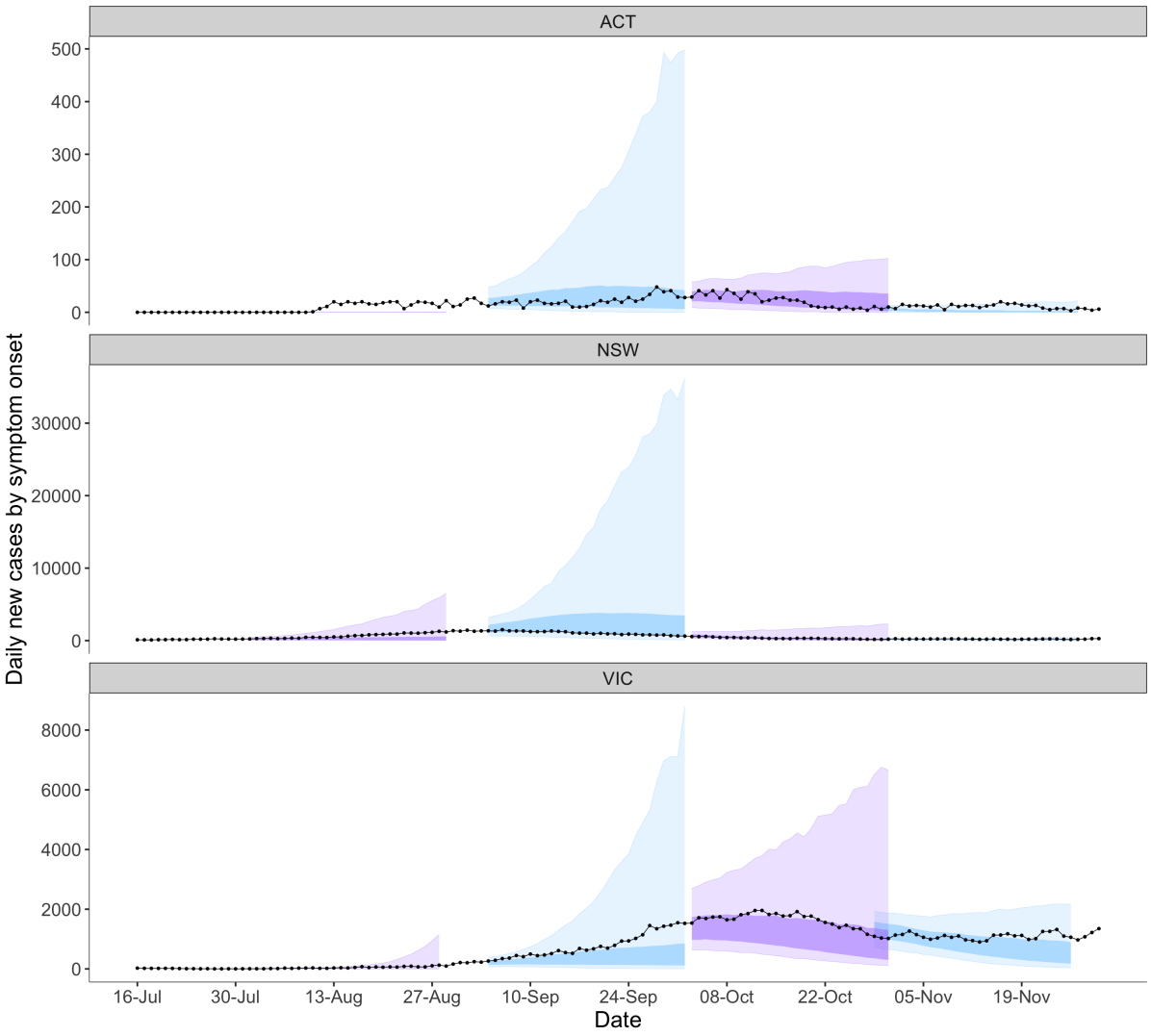

Figure 11: As in Figure 11, but with truncated y-axis limits to zoom in on observed case counts and 50% confidence intervals.

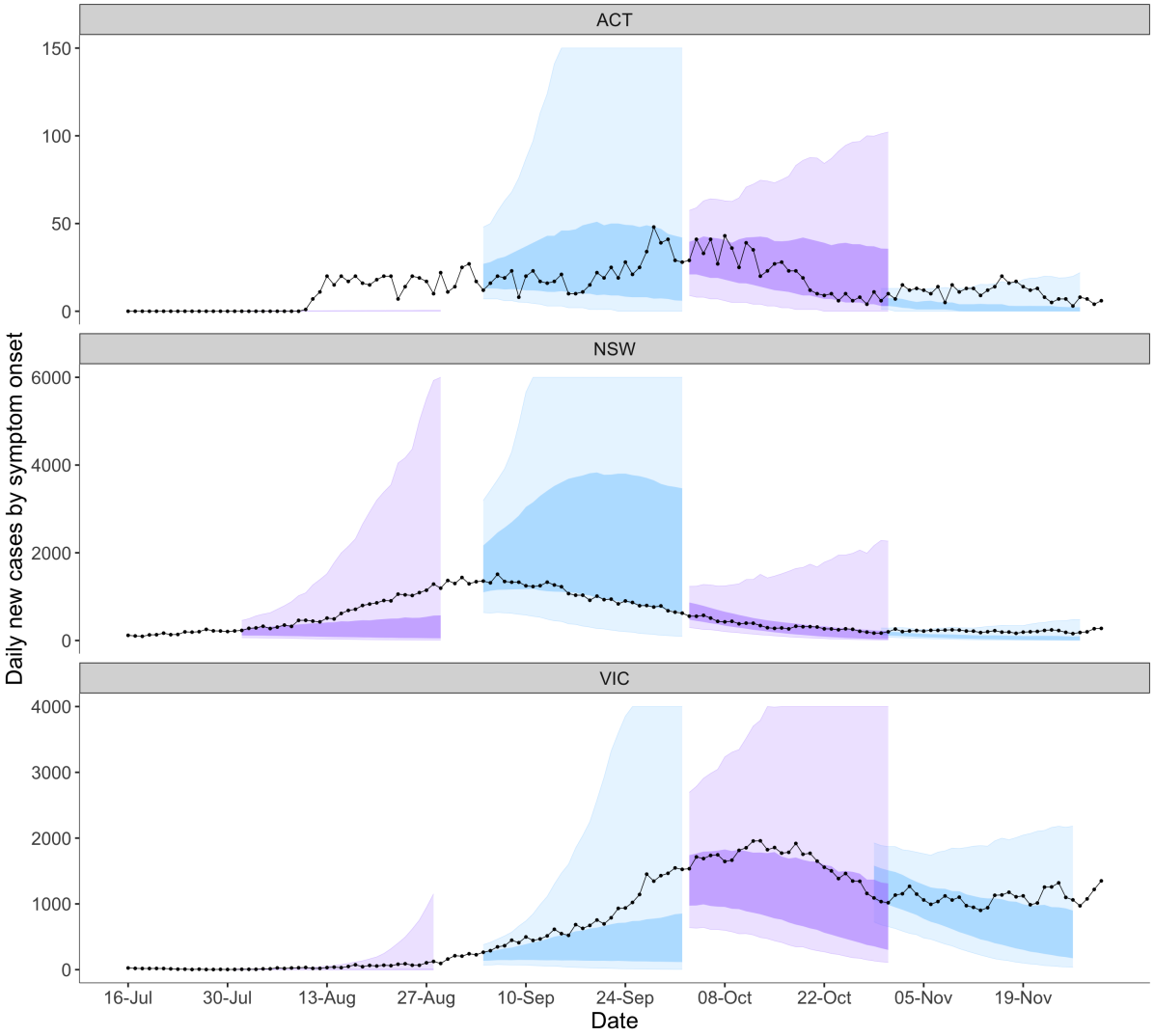

Acknowledgements

This report represents data from the National Notifiable Disease Surveillance System. These data were provided by the Office of Health Protection and Response, Department of Health and Aged Care, on behalf of the Communicable Diseases Network Australia as part of the nationally coordinated response to COVID-19.

We thank public health state from incident emergency operations centres in state and territory health departments, and the Australian Government Department of Health, along with state and territory public health laboratories. We thank members of CDNA for their feedback and perspectives on the results.

We also thank members of state epidemiological units for their support.

Appendix

For methodological details on the mobility, distancing, R_{eff} and forecasting analyses please refer to our previous Technical Report (15 March 2021) available at the following link:

https://mspgh.unimelb.edu.au/__data/assets/pdf_file/0004/4230643/2021-03-15-Technical-report-public-release.pdf

And the following pre-print:

https://www.medrxiv.org/content/10.1101/2021.11.28.21264509v1

Updates made since the preparation of these publications are detailed below.

A Supplementary forecast figures

Figure S1: **14-day projections of new daily local cases** of COVID-19 from the forecasting ensemble for ACT, NSW, and VIC plotted every two weeks from early July to late November 2021 (alternate 14-day periods coloured in purple and blue; darker shading = 50% confidence intervals; lighter shading = 90% confidence intervals). Observed daily counts of locally acquired cases are also plotted from 15 July to 1 December 2021 by date of symptom onset (black dots and lines), based on data extracted from NNDSS on 1 March 2022. Forecasts were fitted to data extracted at the time of analysis (not shown). Due to the time required to update forecasting models to incorporate vaccination, no forecasts were produced in the week commencing 30 August 2021. Due to events such as public holidays, data delays, *etc.*, the forecast start day shifts from week to week, which is why the overlap between forecasts varies. Note that every other forecast are shown here, with the other set displayed in Figure 9.

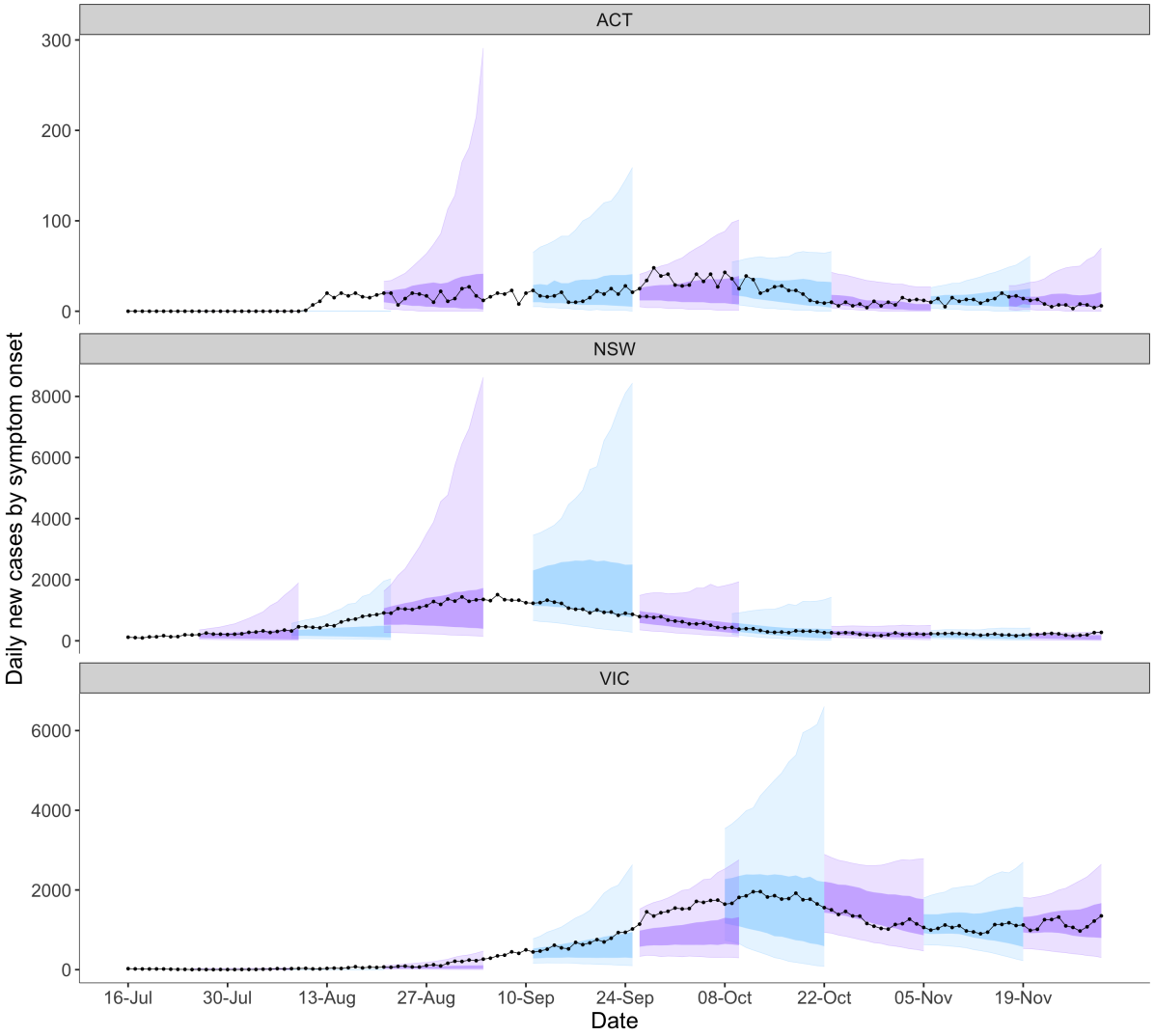

Figure S2: **28-day projections of new daily local cases** of COVID-19 from the forecasting ensemble for ACT, NSW, and VIC plotted every month from early July to late November 2021 (alternate 28-day periods coloured in purple and blue; darker shading = 50% confidence intervals; lighter shading = 90% confidence intervals). Observed daily counts of locally acquired cases are also plotted from 15 July to 1 December 2021 by date of symptom onset (black dots and lines), based on data extracted from NNDSS on 1 March 2022. Forecasts were fitted to data extracted at the time of analysis (not shown). Due to the time required to update forecasting models to incorporate vaccination, no forecasts were produced in the week commencing 30 August 2021. Due to events such as public holidays, data delays, *etc.*, the forecast start day shifts from week to week, which is why the overlap between forecasts varies. Note that every fourth forecast is shown here with plots of other forecasts displayed in Figures 10, S3, and S4.

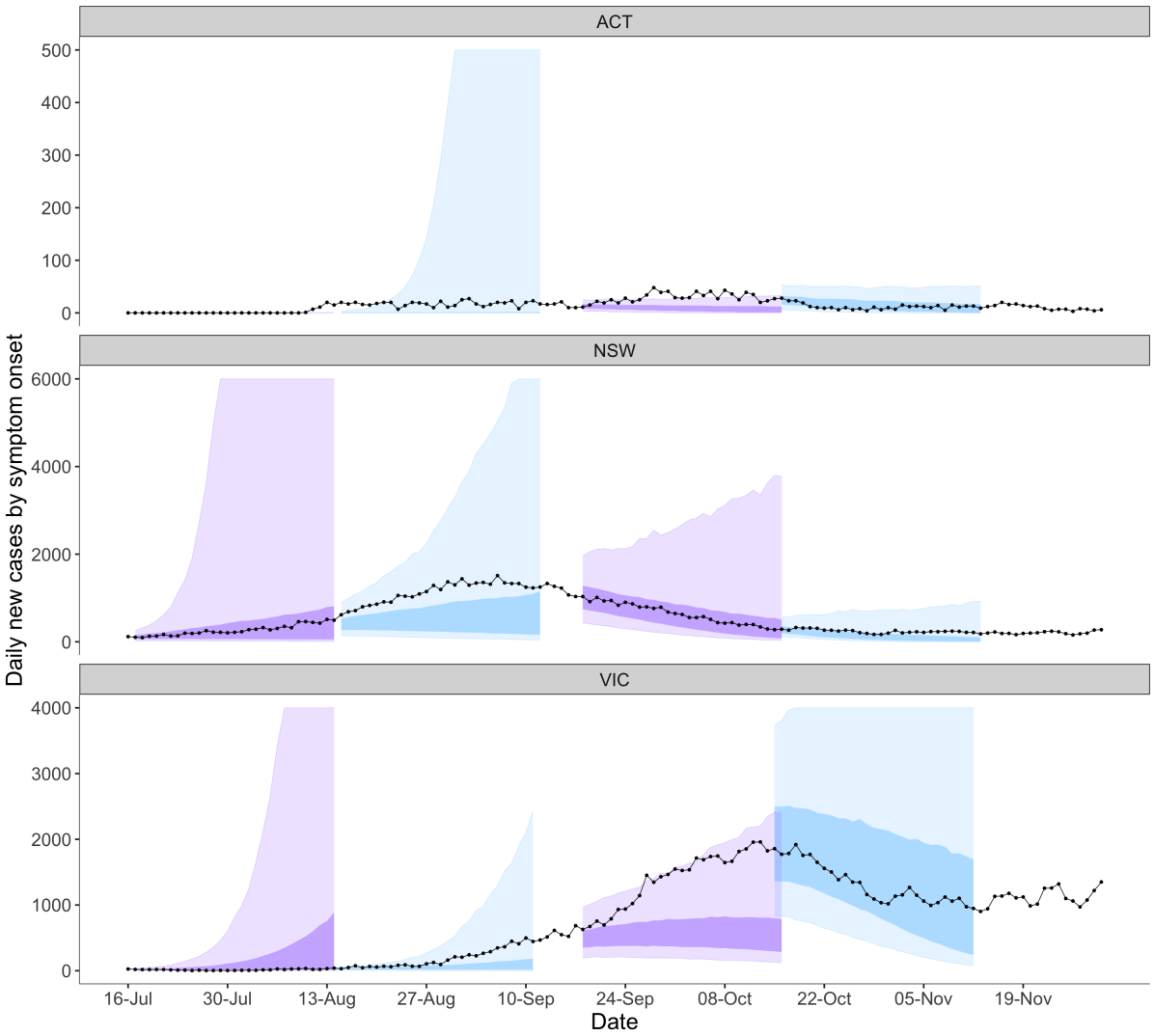

Figure S3: **28-day projections of new daily local cases** of COVID-19 from the forecasting ensemble for ACT, NSW, and VIC plotted every month from early July to late November 2021 (alternate 28-day periods coloured in purple and blue; darker shading = 50% confidence intervals; lighter shading = 90% confidence intervals). Observed daily counts of locally acquired cases are also plotted from 15 July to 1 December 2021 by date of symptom onset (black dots and lines), based on data extracted from NNDSS on 1 March 2022. Forecasts were fitted to data extracted at the time of analysis (not shown). Due to the time required to update forecasting models to incorporate vaccination, no forecasts were produced in the week commencing 30 August 2021. Due to events such as public holidays, data delays, *etc.*, the forecast start day shifts from week to week, which is why the overlap between forecasts varies. Note that every fourth forecast is shown here with plots of other forecasts displayed in Figures 10, S2, and S4.

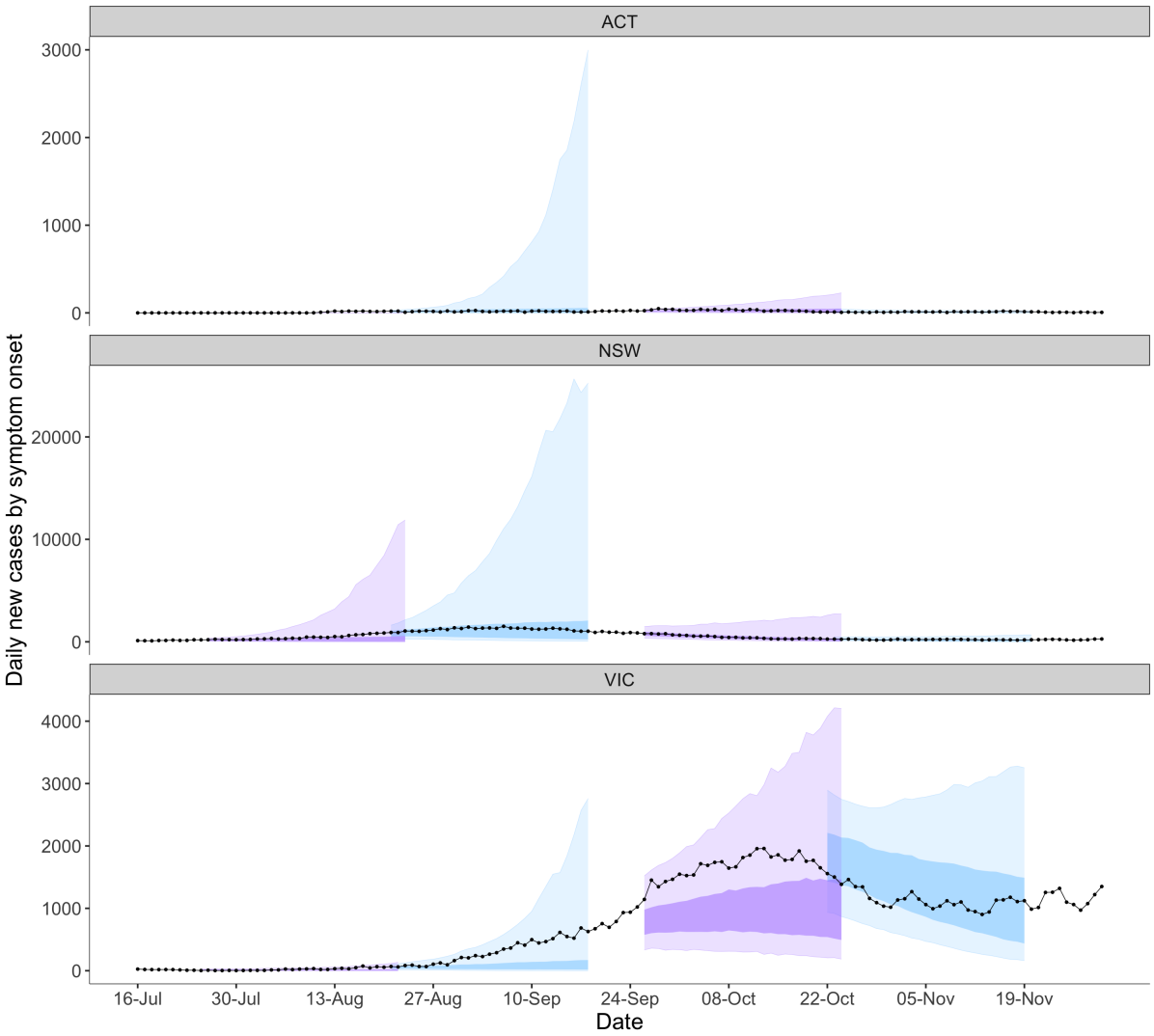

Figure S4: **28-day projections of new daily local cases** of COVID-19 from the forecasting ensemble for ACT, NSW, and VIC plotted every month from early July to late November 2021 (alternate 28-day periods coloured in purple and blue; darker shading = 50% confidence intervals; lighter shading = 90% confidence intervals). Observed daily counts of locally acquired cases are also plotted from 15 July to 1 December 2021 by date of symptom onset (black dots and lines), based on data extracted from NNDSS on 1 March 2022. Forecasts were fitted to data extracted at the time of analysis (not shown). Due to the time required to update forecasting models to incorporate vaccination, no forecasts were produced in the week commencing 30 August 2021. Due to events such as public holidays, data delays, *etc.*, the forecast start day shifts from week to week, which is why the overlap between forecasts varies. Note that every fourth forecast is shown here with plots of other forecasts displayed in Figures 10, S2, and S3.

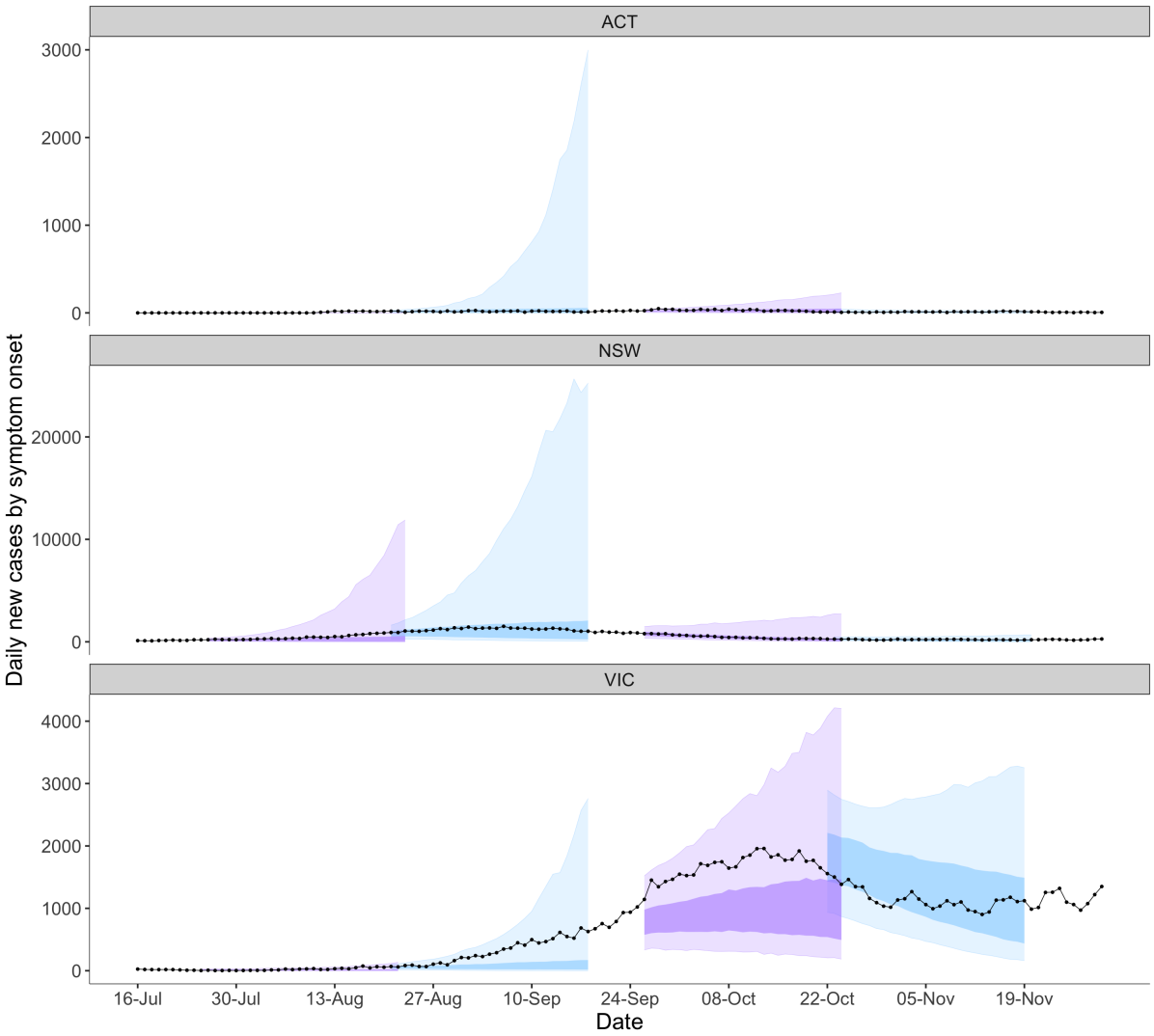

B Accounting for the effect of vaccination on transmission potential

B.1 Overview

We compute the multiplicative effect of vaccination on Component 1 (state-wide transmission potential) of our model of SARS-CoV-2 transmissibility using a simple age structured next-generation matrix model and weekly data on contemporary vaccination coverage in the Australian population from the Australian Immunisation Register (AIR).

Vaccines can impact on multiple elements of transmission and disease (*e.g.*, on susceptibility to infection, probability of onward transmission, *etc*). Our model incorporates a combined effect of protection against infection and onward transmission (assuming infection with the Delta variant) of vaccinated individuals by vaccine product and dose number (See Table S1). Further, we assume a 21-day delay to full protection from a single dose, and a 14-day delay to protection from a second dose (increasing linearly immediately upon vaccination) and that protection does not wane.

Figure 3 presents the estimated multiplicative effect on transmission potential through time by state/territory.

Table S1: Vaccine effectiveness parameters for the Delta variant, based on evidence as of 11 October 2021.

	Reduction in:		Calculated overall
Vaccine	Infection	Onward transmission	reduction in transmission
AstraZeneca dose 1	46%	2%	47%
AstraZeneca dose 2	67%	36%	79%
Comirnaty/Pfizer dose 1	57%	13%	63%
Comirnaty/Pfizer dose 2	80%	65%	93%

B.2 Data

To estimate the effect of vaccination on transmission potential, we use data on vaccine coverage by age, dose number, product (AstraZeneca and Comirnaty/Pfizer), and state/territory from the Australian Immunisation Register.

B.3 Model

We compute the multiplicative effect of vaccination on transmission potential using a simple age structured next-generation matrix model. This enables us to capture the effect of heterogeneous (across ages) vaccination coverage on transmission potential, which captures average transmission rates across the whole population.

We calculate the vaccination-adjusted Component 1 estimate $R^*_{i,t}$ in each state/territory i at each time t as the product of the previous Component 1 estimate $R_{i,t}$ and the vaccination effect at the same time and state $V_{i,t}$:

$$R^*_{i,t} = R_{i,t} V_{i,t} \tag{1}$$

With no vaccination $V = 1$, and as vaccination coverage increases, V approaches $1 - E$, where E is the proportion of onward transmission events prevented by vaccination. With complete vaccination coverage and a vaccine effectiveness of 100% at preventing either acquisition (sterilising immunity) or onward transmission, V would equal zero. We compute $V_{i,t}$ prior to estimating transmission potential, using:

- estimates of vaccination coverage $pV_{a,i,t}$ (described in Equation 6 below) in each age group a, state i, and time t;
- estimates of average vaccine effectiveness $\bar{E}_{a,i,t}$ in each age group a, state i, and time t; and
- an age-structured pre-pandemic next-generation matrix $\mathbf{A}$ representing the expected number of onward infections between each pair of age groups, in the absence of vaccination or any other interventions.

We compute $\mathbf{A}$ from an pre-pandemic age-structured contact matrix for Australia $\mathbf{C}$ [1] which has elements giving the rate of close contacts per unit time between pairs of age groups. We first adjust the number of contacts by a relative infectiousness vector $\mathbf{q}$, where each element q_a gives the relative infectiousness of infected people in each age group a (relative to the age group with the highest rate of transmission, for which $q_a = 1$). We then multiply the resulting matrix by a scalar m; the number of onward infections per relative-contact to obtain the next-generation matrix in the absence of vaccination or other interventions. We determine m by setting the dominant eigenvalue of $\mathbf{A}$, denoted $\rho(\mathbf{A})$, to an estimate of the basic reproduction number R_0 of SARS-CoV-2, and solving for m by numerical optimisation:

$$A_{a',a} = C_{a',a} q_a m \tag{2}$$

$$\rho(\mathbf{A}) = R_0 \tag{3}$$

We then compute the dominant eigenvalue of this hypothesised matrix (the expected reproduction number in the presence of this level of vaccination coverage, but no other interventions or behavioural changes), and the ratio of that eigenvalue to R_0:

$$A^*_{a',a,i,t} = A_{a',a} pV_{a,i,t} \bar{E}_{a,i,t} \tag{4}$$

$$V_{i,t} = \rho(\mathbf{A}^*_{i,t})/R_0 \tag{5}$$

The age-specific vaccination coverage $pV_{a,i,t}$ in each state i and time t is given by the ratio of the cumulative number of people having received a vaccine $nV_{a,i,t}$ in each age group a, state i, and time t, divided by the number of residents $n_{a,i}$ of that age group and state. The average vaccine effectiveness $\bar{E}_{a,i,t}$ is given by the average estimated effectiveness of vaccines $E_{p,d}$ from provider p, after d doses, weighted by the proportion of the vaccinated population in that state and time having received each vaccine product and dose number.

$$pV_{a,i,t} = nV_{a,i,t}/n_{a,i} \tag{6}$$

$$\bar{E}_{a,i,t} = \frac{1}{nV_{a,i,t}} \sum_p \sum_d E_{p,d} nV_{p,d,a,i,t} \tag{7}$$

This approach assumes that the reduction of R_{eff} due to vaccination is the same under pre-pandemic conditions as under post-pandemic restrictions and behaviours. In reality, the effectiveness of vaccination will fluctuate over time as behavioural patterns and contact networks change.

C Estimating the relative transmissibility of the Alpha and Delta variants

C.1 Methodology

In January 2021, we used the below approach to estimate the relative transmissibility of Alpha variant compared to ancestral lineages. In June 2021, we updated this earlier work to jointly

estimate the relative transmissibility of the Alpha and Delta variants compared to ancestral lineages, and to account for variability in relative transmissibility between high-restriction and low-restriction scenarios. We sought to directly estimate the impact of Alpha and Delta on the probability of transmission to a contact per unit of contact time. A change to this parameter is consistent with the hypothesis that the increased growth rates in cases associated with some variants of concern (VOCs) are due to increased viral shedding during infection. With an estimate of this parameter, we can modify our estimates of transmission potential in Australia, whilst accounting for estimated changes to the fraction of contacts that are made with household members, the duration of time spent in the household, and changes to micro-distancing behaviours. We estimated this key parameter by adapting the mathematical model of household and non-household transmission that forms part of our routine methodology for estimating transmission potential in Australia, and fitting it to data from Public Health England. Data were on on secondary attack rates among contacts for Alpha and non-VOCs in nine English regions in one period from November 2020 to January 2021, and household secondary attack rates among household contacts for Alpha and Delta in England nationally over a second period from March to May 2021.

Of note, our analysis assumes that the risk of reinfection is the same for Alpha and Delta (given prior infection with Alpha or ancestral virus). Public Health England reported in their 23 July 2021 risk assessment of Delta that "pseudovirus and live virus neutralisation using convalescent sera from first wave and Alpha infections shows a reduction in neutralisation. National surveillance analysis, adjusted for different variables including age and vaccination, shows a preliminary signal of increased risk of reinfection with Delta compared to Alpha. Further investigations are being undertaken"[8].

C.1.1 Effect of Variants of Concern Alpha and Delta

In the first time period we model the effect of the Alpha variant relative to wild-type on per-unit-contact time probability of transmission via a parameter for the power of the probability of not transmitting per unit of contact time:

$$p_{1\alpha} = 1 - (1 - p_{1wt})^{\phi_{\alpha:wt}} \tag{8}$$

where $p_{\alpha 1}$ and p_{wt1} are the per-unit-contact time probabilities of transmission for the Alpha variant and non-VOCs ("ancestral"), respectively, in the first time period, and $\phi_{\alpha:wt}$ is a free parameter that controls the relative infectiousness between them.

We expected that there may be differences in the per-unit-time probabilities of transmission between the two time periods due to changes in immunity through vaccinations and exposures, so model the effect of the Alpha and Delta variants in the second period as:

$$p_{2\alpha} = 1 - (1 - p_{1\alpha})^{\phi_{period2}} \tag{9}$$

$$p_{2\delta} = 1 - (1 - p_{2\alpha})^{\phi_{\delta:\alpha}} \tag{10}$$

where $p_{\alpha 2}$ and $p_{\delta:\alpha}$ are the per-unit-contact time probabilities of transmission for the Alpha and Delta variants, respectively, in the second time period, and $\phi_{period2}$ representing the relative infectiousness between the second and first time periods, and $\phi_{\delta:\alpha}$ represents the relative infectiousness between the Delta and Alpha variants. All values of ϕ are constrained to be positive, and a value of any $\phi = 1$ would imply that the two variants have the same transmissibility.

[8] https://www.gov.uk/government/publications/investigation-of-sars-cov-2-variants-of-concern-variant-risk-assessments

C.1.2 Model for household and non-household attack rates

Our existing transmission potential model[9] explicitly considers secondary attack rates among household members and non-household members, modelled as a function of: the probability of transmission per unit contact time; the average duration of contacts with household and non-household members; and modification of the non-household attack rate. The latter is a combined effect of reductions in the per-unit-contact-time transmission probability and in the average duration of non-household contacts.

We explicitly model the household secondary attack rate at location i, time period j, and variant k as:

$$HSAR_{ijk} = 1 - (1 - p_{jk})^{HD_{ij}} \tag{11}$$

where p_{jk} is the probability of transmission per unit of contact time, and HD_{ij} is the average duration of household contacts at place i in period j, summed over the full course of infection. We model the secondary attack rate for non-household members as:

$$OSAR_{ijk} = \gamma_{ij} \times (1 - (1 - p_{jk})^{OD_0}) \tag{12}$$

where OD_0 is the average duration of non-household contacts per 24 hours at baseline (prior to the pandemic and restrictions), and γ_{ij} is the reduction in non-household secondary attack rates as a function of micro-distancing behaviour in location i in period j. We infer the parameters HD_{ij} and γ_{ij} from data on mobility and behavioural change as:

$$HD_{ij} = HD_0 \times h_{ij} \tag{13}$$

$$\gamma_{ij} = 1 - \beta \times d_{ij} \tag{14}$$

where HD_0 is the average duration of household contacts over the full infectious period at baseline, h_{ij} is proportional change in the amount of time spent in the household, inferred from the Google mobility metric 'Time at Residential', d_{ij} is the degree of adherence of micro-distancing behaviour, scaled to range from 0 at baseline to 1 at the peak of micro-distancing, and β is a free parameter controlling the impact of micro-distancing on reducing non-household transmission that is fitted to Australian case data.

C.1.3 Fitting to UK attack rate data

We use data from two of Public Health England's (PHE) series *Investigation of SARS-CoV-2 Variants of Concern: Technical Briefings* (`https://www.gov.uk/government/publications/investigation-of-novel-sars-cov-2-variant-variant-of-concern-20201201`):

- Technical Briefing 5, Table 4, reports numbers of contacts of cases with the **Alpha variant and non-VOCs**, and the number of those contacts that became cases, **in nine English regions between 2020/11/30 and 2021/01/10**, and
- Technical Briefing 15, Table 10, reports numbers of contacts of cases with the **Delta and Alpha variants**, and the number of those contacts that became cases, **nationally in England between 2021/03/29 and 2021/05/19**.

For the first period, our model separately considers attack rates for the Alpha variant and non-VOCs in each of these regions, using region-specific estimates of mobility, micro-distancing, and macro-distancing. By considering all nine regions as independent observations (rather than

[9] `https://doi.org/10.1101/2021.11.28.21264509`

aggregating the data for all of England), we increase statistical power and consider the effect of the variant at different levels of restrictions. The fact that we see similar estimates of attack rates across all nine regions gives us confidence that higher attack rates are due to biological differences between variants rather than founder effects or confounding with outbreaks in specific settings.

Unfortunately, these attack rate data are not dis-aggregated by whether or not the contacts were household members. We must therefore adapt our model to estimate an overall attack rate over contacts, and adjust it for non-random ascertainment of contacts in the PHE dataset.

We can estimate the overall secondary attack rate for each region in the first period for the Alpha variant and non-VOCs SAR_{i1k} as a combination of household and non-household secondary attack rates weighted by w_{i1}, the fraction of contacts that are household members in that period:

$$SAR_{i1k} = w_{i1} \times HSAR_{i1k} + (1 - w_{i1}) * OSAR_{i1k} \tag{15}$$

$$w_{i1} = HC/(HC + OC_{i1} * ID) \tag{16}$$

where HC is the average number of household contacts (assumed the same for each region), OC_{i1} is the average number of non-household contacts per 24 hours, and ID is the average duration of infectiousness in days. Our model assumes that household contacts stay the same throughout the course of infection, but that there is a different set of non-household contacts on each day.

The overall secondary attack rates estimated by this model correspond to the average number of contacts specified as HC and OC_i. Whilst the number of household contacts is likely to be consistent between analyses, the operational contact definition used by the contact tracing teams that provided the PHE data is likely to yield a smaller number of contacts than the contact surveys used to estimate OC_i. Moreover, the number of contacts will not be a random sample of the larger number of contacts, since operational contact tracing will target those individuals with a greater risk of transmission. The consequence of this is that observed attack rates are biased upwards. This will also affect estimates of the relative transmissibility of the Alpha variant from these raw data — reducing the apparent transmissibility. We account for these issues by introducing a free parameter ψ to relate the 'true' and observed attack rates by raising the true attack rate to the power of ψ: SAR_{ijk}^{ψ}.

For the second time period we do not have data dis-aggregated by region, however the data are dis-aggregated by which contacts are household contacts or not. While this spatial aggregation is likely to reduce the statistical power of our model, we expect that the identified number of contacts from households is likely to be more accurate than the identified number of non-household contacts. Therefore, for the second time period, our model was fit only to estimate household secondary attack rates for the Alpha and Delta variants using mobility data, and did not estimate non-household nor overall secondary attack rates for this period.

C.1.4 Full model

We specified a Bayesian statistical model to estimate ϕ and the other parameters from UK attack rate data as follows:

$$C_{i1wt} \sim Binomial(N_{i1wt}, SAR^{\psi}_{i1wt}) \tag{17}$$
$$C_{i1\alpha} \sim Binomial(N_{i1\alpha}, SAR^{\psi}_{i1\alpha}) \tag{18}$$
$$C_{n2\alpha} \sim Binomial(N_{n2\alpha}, HSAR_{n2\alpha}) \tag{19}$$
$$C_{n2\delta} \sim Binomial(N_{n2\delta}, HSAR_{n2\delta}) \tag{20}$$
$$SAR_{i1wt} = w_{i1} \times HSAR_{i1wt} + (1 - w_i) \times OSAR_{i1wt} \tag{21}$$
$$SAR_{i1\alpha} = w_{i1} \times HSAR_{i1\alpha} + (1 - w_i) \times OSAR_{i1\alpha} \tag{22}$$
$$w_{i1} = HC/(HC + OC_{i1} \times ID) \tag{23}$$
$$HSAR_{i1wt} = 1 - (1 - p_{1wt})^{HD_{i1}} \tag{24}$$
$$HSAR_{i1\alpha} = 1 - (1 - p_{1\alpha})^{HD_{i1}} \tag{25}$$
$$HSAR_{n2\alpha} = 1 - (1 - p_{2\alpha})^{HD_{n2}} \tag{26}$$
$$HSAR_{n2\delta} = 1 - (1 - p_{2\delta})^{HD_{n2}} \tag{27}$$
$$OSAR_{iwt} = \gamma_{i1} \times \left(1 - (1 - p_{1wt})^{OD_0}\right) \tag{28}$$
$$OSAR_{i\alpha} = \gamma_{i1} \times \left(1 - (1 - p_{1\alpha})^{OD_0}\right) \tag{29}$$
$$HD_{i1} = HD_0 * h_{i1} \tag{30}$$
$$HD_{n2} = HD_0 * h_{n2} \tag{31}$$
$$\gamma_{i1} = 1 - \beta * d_{i1} \tag{32}$$
$$\tag{33}$$

where N and C are the number of contacts, and the number of those contacts that became cases in either each English region i, or nationally n, subscripts 1 and 2 correspond to the first and second data periods, and wt, α, and δ correspond to non-VOCs, or the Alpha or Delta variants, respectively. The model was fitted by MCMC using the same algorithm and software as the model for R_{eff}. The model was run until there were at least 1000 effective samples of each parameter. Convergence was assessed visually and by the potential scale reduction factor or $\hat{R}$ (less than 1.01 for all parameters). Calibration of the model was assessed by posterior predictive checks over each of C, and the empirical estimate of the ratio of attack rates between variants for each region: $\frac{C_{i1\alpha}/N_{i1\alpha}}{C_{i1wt}/N_{1wt}}$ for non-VOCs and the Alpha variant in the first period, and nationally between the Alpha and Delta variants in the second period $\frac{C_{i1\delta}/N_{i1\delta}}{C_{i1\alpha}/N_{1\alpha}}$, and these indicated good fit.

C.1.5 Parameter values and prior distributions

When fitting the transmission potential model for Australia, the parameters OC_{i1} (non-household contacts per 24 hours), h_{ij} (relative time spent at home), and d_{i1} (relative micro-distancing effect) are all informed by bespoke statistical models tailored to the Australian situation and surveys carried out only in Australia. We developed equivalent estimates of these parameters for the UK from a range of other sources.

To estimate OC_{i1} we used the macro-distancing model fitted to Australian contact survey data to predict the number of non-household contacts per days in each English region, based on the values of Google mobility metrics for those regions. Google mobility data were downloaded for each English county, aggregated up to compute the average value over each region,

and then averaged for each region over the period over which attack rate data were collected. Predictions of the Australian contact model were visually compared with summary statistics of non-household contact rates from April to August 2020 as estimated by the UK's CoMix survey series and found to have good calibration.

We used the aggregated estimate of change in Google's time at residential to inform h_{ij}.

To estimate d_{i1}, we analysed data on adherence to the UK's 2m rule using data for each English region from regular YouGov behavioural surveys conducted in partnership with Imperial College London. We calculated the number of people responding that they had not broken the 2m rule ("come into physical contact with (within 2 meters / 6 feet)") in the past seven days. This is analogous to the 1.5m rule question used to define our micro-distancing metric in Australia. This time series was analysed using a Binomial Generalised Additive Model (GAM) to estimate a time-series of the metric for each region over the course of the pandemic. This time-series was re-scaled to have maximum value 1 and then averaged over the time period over which attack rate data were collected.

The model comprised eight parameters; four for which we have existing estimates (p_{1wt}, HC, HD_0, and OD_0) and four for which we do not ($\phi_{\alpha:wt}$, $\phi_{\delta:\alpha}$, $\phi_{period2}$ and ψ). We defined an informative prior for p_{1wt} based on a normal approximation to the posterior for this parameter from the Australian R_{eff} model. This assumes *a priori* that the non-VOCs in the UK have equivalent infectiousness to the variants that have circulated in Australia to date, though the parameter can be amended by the UK attack rate model fitting procedure if this is inconsistent with the data.

For HC, HD_0, and OD_0, we used the same priors as we use in fitting the Australian model of R_{eff}– based on surveys of contact behaviour in Australian prior to the pandemic. The average number of household contacts in each English region as reported in the YouGov surveys agreed closely with this Australian prior for HC. We chose to use the Australian estimate rather than the UK estimates since the posterior estimate of p_{1wt} was estimated contingent on this distribution.

Values of ϕ and ψ must be positive and a value of 1 indicates no effect (of the variant or of bias in contact acquisition, respectively). We therefore specified minimally informative positive-truncated normal prior distributions for both parameters, with mode (μ parameter of the normal distribution) of 1. For ψ we set the standard deviation of the normal prior distribution, σ, to 1 to allow a large range of values, and for values of ϕ we set it to 1. Prior predictive checks on the ratio of attack rates between Alpha and non-VOCs ($SAR_{i1\alpha}/SAR_{i1wt}$) with this prior on values of ϕ confirmed that the prior was vague with respect to the relative transmissibility of Alpha versus non-VOCs. In other words, multiplicative increases in transmissibility of Alpha estimated from other studies were within the bulk of the prior distribution, as were larger increases and decreases in transmissibility, and likewise Delta relative to Alpha.

β was fixed at the posterior mean as estimated from the Australian model. In the absence of a time series of attack rate data, it is not possible to estimate this parameter independently for the UK, and the value of the parameter is poorly statistically identified in this model due to potential confounding with other parameters – especially ψ. For this reason, uncertainty in β was not considered in this analysis.

D Updates to the SEEIIR Forecast in 2021

In 2021, the SEEIIR model was updated to account for the effects of vaccination on transmission. These updates were introduced into our ensemble model used for reporting in the week commencing 7 September 2021. For a description of the SEEIIR model specified prior to these updates, refer to the March 2021 Technical Report[10].

D.1 Model overview

We used a discrete-time stochastic SEEIIR compartmental model of infection with vaccination to characterise infection in each Australian jurisdiction, with parameters fit to local contexts through a particle filter. The SEEIIR model of SARS-CoV-2 spread assumes that at any given point in time t, $\mathsf{S}(t)$ individuals are *susceptible* to infection, $\mathsf{E_1}(t) + \mathsf{E_2}(t)$ individuals have been *exposed*, $\mathsf{I_1}(t) + \mathsf{I_2}(t)$ individuals are *infectious* and $\mathsf{R}(t)$ individuals have *recovered* and are no longer infectious. We capture the effect of vaccination upon the population by splitting compartments into unvaccinated and vaccinated groups, for example the $\mathsf{S^U}(t)$ unvaccinated and $\mathsf{S^V}(t)$ vaccinated susceptible population. A full compartment transition diagram follows:

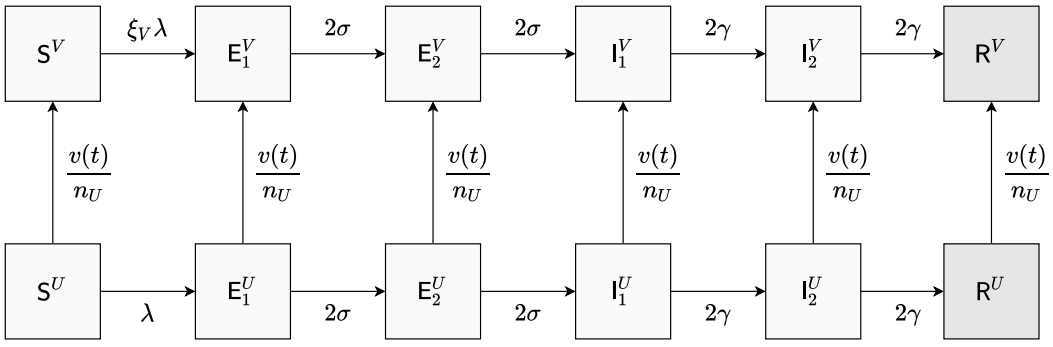

$$\lambda = \beta(\mathsf{I}_1^U + \mathsf{I}_2^U) + \beta\tau_V(\mathsf{I}_1^V + \mathsf{I}_2^V)$$
$$n_U = \mathsf{S}^U + \mathsf{E}_1^U + \mathsf{E}_2^U + \mathsf{I}_1^U + \mathsf{I}_2^U + \mathsf{R}^U$$

Figure S5: The SEEIIR model with vaccination. Transitions between compartments occur according to the rates that are labelled upon each arrow.

Individuals are infected and moved from S to $\mathsf{E_1}$ at a rate proportional to the total force of infection λ. Exposed individuals move from $\mathsf{E_1}$ to $\mathsf{E_2}$ and $\mathsf{E_2}$ to $\mathsf{I_1}$ at rate 2σ, and infected individuals move from $\mathsf{I_1}$ to $\mathsf{I_2}$ and from $\mathsf{I_2}$ to R at rate 2γ. Note that we model these transitions across two compartments to produce a Gamma distribution (with shape 2) of latent and infectious period respectively. The effect of vaccination in reducing susceptibility to infection is modelled captured through the reduction in the force of infection upon the $\mathsf{S^V}$ population by a factor ξ_V. Similarly, the reduced onward transmission of the infected vaccinated population $\mathsf{I_{1,2}^V}$ is captured in a reduction of their contribution towards the total force of infection by the factor τ_V.

[10] https://mspgh.unimelb.edu.au/__data/assets/pdf_file/0004/4230643/2021-03-15-Technical-report-public-release.pdf

Parameters are estimated over time using a particle filter model as described in previous work by Moss et al. on forecasting influenza ([2, 3]). For every jurisdiction, 2,000 particles simulating the SEEIIR process are produced, with repeated re-sampling of particles and their associated parameter sets according to the likelihood of their produced case incidence. This likelihood is defined by under a population-wide sampling observation model:

$$\begin{aligned} \mathcal{L}(y_t \mid x_t) &\sim \text{NegBin}(\mathbb{E}[y_t], k) \\ \mathbb{E}[y_t] &= (1 - p_{inc}(t)) \cdot bg_{obs} + p_{inc}(t) \cdot p_{obs} \cdot N \\ p_{inc}(t) &= \frac{I_2^{U,V}(t) + R^{U,V}(t) - I_2^{U,V}(t-1) - R^{U,V}(t-1)}{N} \end{aligned} \tag{34}$$

Where $p_{inc}(t)$ is the probability of entering the I_2 compartment, p_{obs} is the observation probability and bg_{obs} reflects the number of expected cases that are not directly subsequent to local epidemic activity.

D.2 Vaccine efficacy calculation

The values for vaccine efficacy are calculated so as to be concordant with the method used in the model of transmission potential (see "Accounting for the effect of vaccination on transmission potential"), with the same values of $nV_{p,d,a,i,t}$ and vaccine efficacy estimates being used here. For each age group a, we calculate the mean efficacy of vaccination within the vaccinated population upon reducing susceptibility $\bar{E}_a^S$ as the sum of estimated efficacy against susceptibility $E_{p,d}^S$ for differing vaccine products p and dose number d weighted by the proportion of vaccinated individuals in the age group a having received that combination. We also produce an estimate for $\bar{E}_a^O$, the total reduction in transmission between vaccinated individuals within an age group in similar fashion, using the estimates of vaccine efficacy against onwards transmission $E_{p,d}^T$:

$$\bar{E}_a^S = \frac{1}{nV_a} \sum_p \sum_d E_{p,d}^S nV_{p,d,a} \qquad \bar{E}_a^O = \frac{1}{nV_a} \sum_p \sum_d (1-(1-E_{p,d}^T)(1-E_{p,d}^S)) nV_{p,d,a}$$

Using a next generation matrix $\mathbf{A}$ (with construction described in the transmission potential vaccination model), we can calculate the multiplicative effect of both $\bar{E}_{a,i,t}^S$ and $\bar{E}_{a,i,t}^O$ in reducing the expected reproduction number of $\mathbf{A}$ across two stages, producing $\mathbf{A}^{*S}$, the next-generation matrix if vaccination only reduced susceptibility and $\mathbf{A}^{*O}$, the next-generation matrix with vaccination reducing both susceptibility and onwards transmission, assuming assortativity:

$$A_{a',a}^{*S} = [1 - pV_{a'} \bar{E}_a^S] A_{a',a} \qquad A_{a',a}^{*O} = [1 - pV_a \bar{E}_a^O] A_{a',a}$$

We can then recover the age-mixing adjusted mean efficacies for vaccination susceptibility reduction and overall transmission reduction as the reduction in the reproduction number between each stage relative to the total proportion of vaccinated individuals pV, where $\rho(\mathbf{X})$ is the dominant eigenvalue of $\mathbf{X}$:

$$\xi = \frac{\rho(\mathbf{A}^{*S})}{\rho(\mathbf{A}) pV} \qquad \tau = \frac{\rho(\mathbf{A}^{*O})}{\rho(\mathbf{A}^{*I}) pV}$$

These calculations are repeated across time t and jurisdiction i with $nV_{p,d,a} := nV_{p,d,a,i,t}$, producing a time series by jurisdiction of $\xi_i(t)$ and $\tau_i(t)$ that is consumed by the compartmental

model. Similarly, the vaccination rate $v_i(t)$ for each jurisdiction is calculated as the daily increase in vaccinated individuals, produced from the weekly increases observed in the AIR data. The values of $\xi_i(t)$ and $\tau_i(t)$ are held constant through the forecasting period, while the value of $v_i(t)$ is predicted into the forecast using simple logistic regression over the proportion of eligible individuals vaccinated, with the regression fit over the last seven days of available data.

D.3 Particle filter parameterisation

The force of infection parameter $\beta_i(t)$ is calculated as the product of $C_{1\cdot2}(t)$ and the inverse of the infectious period $\gamma(t)$, with the expected effect of vaccination removed by dividing through by the reduction in transmission potential attributed to vaccination $V_{i,t}$, so as to avoid double-counting this effect.

$$\beta_i(t) = \frac{C_{1\cdot2}(t)}{V_{i,t}} \cdot \gamma(t)$$

Where the $C_{1\cdot2}$ trajectory used by each particle is selected from a set of 1,000 time series provided by the transmission potential/effective reproduction number model. Selection occurs according to the inferred parameter R_{ix}, with each particle using the $C_{1\cdot2}$ trajectory with the respective rank equal to R_{ix}, where this ranking is recalculated at each step of the re-sampling process.

Table S2: Parameter values for (i) the transmission model; (ii) the observation model; and (iii) the bootstrap particle filter.

		Description	Value
(i)	N	The population size	Table S3
	σ	The inverse of the latent period (days^{-1})	See text
	γ	The inverse of the infectious period (days^{-1})	See text
	R_{ix}	The index of the $C_{1\cdot2}$ trajectory	$U(1, 1000)$
	τ	The time of the initial exposures (days)	$U(0, 50)$
(ii)	bg_{obs}	The background observation rate	0.05
	p_{obs}	The observation probability	0.8
	k	The dispersion parameter	10
(iii)	N_{px}	The number of particles	2000
	N_{min}	The minimum number of effective particles	$0.25 \cdot N_{px}$

Parameters σ and γ were sampled from a multivariate log-normal distribution that was defined to be consistent with a generation interval with mean=4.7 and sd=2.9. Population sizes are projected state-wide counts of individuals of any age.

E Updates to the Probabilistic Forecast in 2021

In 2021, a number of updates were made to the Probabilistic model. For a description of the Probabilistic model prior to these updates, refer to the March 2021 Technical Report[11].

[11] https://mspgh.unimelb.edu.au/__data/assets/pdf_file/0004/4230643/2021-03-15-Technical-report-public-release.pdf

Table S3: The population sizes used for each forecast.

State	Population
Australian Capital Territory	431,124
New South Wales	8,167,576
Northern Territory	246,741
Queensland	5,185,508
South Australia	1,770,799
Tasmania	541,248
Victoria	6,681,838
Western Australia	2,667,231

E.1 Revisions to the transmissibility function

The transmissibility function was revised to include the effects of variants of concern (VOCs) and vaccines. The revised local component of transmissibility is

$$R_L^{(2)}(t) = C(t)V(t)R_L(t)$$

where the $C(t)$ and $V(t)$ are multipliers on the local transmissibility, $R_L(t)$, as defined in the March 2021 Technical Report[12].

E.2 Incorporating the effect of VOCs

The VOC effect $C(t)$ is incorporated into the model to allow for an increase in transmissibility attributable to variants as follows

$$C(t) = \begin{cases} 1, & t < 28/01/2021 \\ c_\alpha, & 28/01/2021 \leq t < 01/05/2021 \\ c_\delta, & t \geq 01/05/2021 \end{cases}$$

where the multipliers c_α and c_δ (inferred) are for the α (Alpha) and δ (Delta) variants, respectively, and have priors given by

$$c_\alpha \sim 1 + \text{Gamma}(0.4^2/0.075, 0.075/0.4)$$
$$c_\delta \sim 1 + \text{Gamma}(1.1^2/0.075, 0.075/1.1).$$

E.3 Incorporating the effect of vaccines

Population average vaccine effects (vaccine factor or VF) were provided as an output from the model described in Section B.3 ($v_c(t)$) as a multiplier on transmissibility due to vaccination. We include this effect as a multiplier on transmissibility but account for a period of heterogeneity in vaccine coverage in the early phase of the vaccine roll-out. We consider heterogeneity in the VF prior to 20/08/2021 which is captured through the model

$$V(t) = \begin{cases} p + (1-p)v_c(t), & t < 20/08/2021 \\ pe^{-r(t-20/08/2021)} + (1 - pe^{-r(t-20/08/2021)})v_c(t), & t \geq 20/08/2021 \end{cases}$$

[12] https://mspgh.unimelb.edu.au/__data/assets/pdf_file/0004/4230643/2021-03-15-Technical-report-public-release.pdf

where p is a mixture parameter (that can be interpreted as the proportion of cases occurring in sub-populations with relatively low vaccination coverage compared to the general population), and v_c is the estimated vaccine efficacy, assuming homogeneous case incidence relative to vaccine coverage, as estimated in Section B.3. The parameter p is estimated as part of our Stan fitting procedure, with a Beta$(2, 7)$ prior, which has mean $p = 0.22$; the parameter is estimated separately for NSW, due to clearly identified heterogeneity in the period used for fitting, and for other jurisdictions collectively to allow for potential heterogeneity.

To reflect the early targeting of vaccination campaigns in LGAs of concern and subsequent reduction in vaccine coverage heterogeneity as coverage increases overall, we assume that heterogeneity decays exponentially over time such that it is effectively homogeneous vaccine coverage 28 days after 20/08/2021. This decay in heterogeneity is captured by the exponential term multiplying the mixture parameter p. The rate parameter r of this decay is inferred assuming a Log-Normal$(\log(0.16), 0.1)$ prior chosen such that the mean time for the return to homogeneous VF is approximately 28 days.

In other words, we assume that epidemic activity becomes more distributed among individuals representative of the general population over time.

E.4 Forecasting the vaccine factor

We forecast the VF by using the supplied estimates (from Section B.3) and applying a random walk with drift, similar to how we forecast the mobility and micro-distancing effects for this forecasting model. Over the forecast horizon, we assume a maximum VF reduction of 0.3 or the minimum VF observed across jurisdictions (whichever is lower) as the lower limit.

E.5 Updates to epidemiological assumptions

We adjusted the reporting delay for our model by fitting a Gamma distribution to the time from symptom onset to confirmation. The fitted shape and scale parameters are 1.28 and 2.31 respectively. We also updated our generation interval to be a Gamma distribution with shape 2.75 and scale 1.00. The dispersion parameter k was revised upwards from 0.1 to 0.15.

E.6 Case ascertainment

Detection probabilities were updated such that the probability of detection of a symptomatic case is 0.950 for all jurisdictions. The probability of detection of an asymptomatic case is 0.150 for all jurisdictions. This choice results in an overall probability of detecting a local case of 0.695. The probability of detecting an imported case is 0.980 for all jurisdictions.

E.7 Conditioning on data in the generative model

In the generative model, we overhauled how a forecast trajectory is deemed to be consistent (or not) with the observed cases. We consider 20 day periods whereby the minimum number of allowable cases in each interval is 0.3 times the observed cases in the window and the maximum number of allowable cases in the interval is 2.5 times the observed cases. In the 14 days preceding the forecast date, we tighten the lower and upper limits to 0.5 and 1.5 respectively, upweighting the effect of the most recent data on forecast $R_L(t)$ trajectories (local transmissibility).

E.8 Estimating transmissibility for imported cases

We updated our approach for estimating the transmissibility for imported cases, R_I, to account for the vaccination of hotel quarantine workers. In the absence of data on vaccination coverage

of hotel quarantine workers, we assumed levels of coverage in this group to be > 90% across states/territories (see below).

The updated model introduces distributions for two parameters: $p_{v,h}$, to approximate the proportion of hotel quarantine workers vaccinated, and $v_{e,h}$, to approximate the overall vaccine effectiveness. While both parameters have support between 0 and 1, the proportion of hotel quarantine workers vaccinated ($p_{v,h}$) is assumed to be distributed as a Beta(280,22) random variable (so most likely values are in the range from 90% to 99%, with a mode at 93%) and the overall vaccine effectiveness ($v_{e,h}$) is distributed as a Beta(73,9) random variable (so most likely values are between 83% and 97%, with a mode of 90%) in line with evidence on vaccine effectiveness at the time.

Combining these new parameters with the original fitted transmissibility of imported cases, we have the transmissibility for imported cases of $R_I \times (1–p_{v,h} \times v_{e,h})$.

F Update to the Time-Series Forecast in 2021

In the week's commencing 8 March, 14 June, and 25 October 2021, the Time-series forecast model was re-calibrated using up-to-date data from the John Hopkins COVID19 repository (more locations and more dates). Like the previous models, the updated model was an AR(24). The value of $p = 24$ is chosen to minimize the average 14-day-ahead mean absolute error on recent Australian data and data from 30 comparable countries (so 24 model parameters, estimated from approximately 10^4 daily observations).

Of note, in the week commencing 25 October, the model was updated with a refined transformation that more precisely described the exponential nature of global cases growth at the time. The parameters of the GAR(p = 24) model were re-estimated with the latest data from 30 comparable countries with this updated transformation parameter.

G Update to the micro-distancing model as of 29 March 2021

We continued to improve our methods for estimating transmission potential (TP) in 2021. As of the week commencing 29 March 2021, our TP model incorporated an improved micro-distancing model that allows for a step-change (rather than only a smooth transition, as previously and as described in Golding et al[13]) in behavioural data streams on dates when physical distancing policies were implemented, and when short-term policies (< 1 week) were lifted.

The previous statistical model was useful to describe behaviour early in the epidemic (*e.g.*, during and after national restrictions in March/April 2020), but was less able to capture the complexity of the varying restrictions and behavioural changes in the subsequent period. We have replaced this model with a simpler approach (a generalised additive model) that removes daily noise in responses to surveys on adherence to physical distancing in each state, but responds to policy changes (*e.g.*, short-term stay-at-home restrictions) that are likely to influence micro-distancing behaviours.

[13] https://doi.org/10.1101/2021.11.28.21264509

References

[1] Kiesha Prem, Alex R. Cook, and Mark Jit. Projecting social contact matrices in 152 countries using contact surveys and demographic data. *PLOS Comp Biol*, 13(9):1–21, 2017.

[2] Robert Moss, Alexander E Zarebski, Sandra J Carlson, and James M McCaw. Accounting for healthcare-seeking behaviours and testing practices in real-time influenza forecasts. *Tropical medicine and infectious disease*, 4(1):12, 2019.

[3] Robert Moss, Alexander Zarebski, Peter Dawson, and James M McCaw. Forecasting influenza outbreak dynamics in Melbourne from Internet search query surveillance data. *Influenza and other respiratory viruses*, 10(4):314–323, 2016.